

CHAPTER 4: TESTING OF ENGINEERED SOIL MEDIA FOR PHOSPHORUS ADSORPTION OR DESORPTION

List of Tables	4-ii
List of Figures	4-iii
INTRODUCTION	4-1
MATERIALS AND METHODOLOGY	4-4
Engineered Soil Media Preparation	4-4
Engineered Soil Media Tests	4-4
Modeling	4-7
RESULTS AND DISCUSSION	4-9
Adsorption Equilibrium Isotherm Study	4-9
Adsorption Equilibrium Kinetic Study	4-9
Breakthrough Study	4-10
Desorption Study	4-10
REFERENCES	4-11

List of Tables

Table 1 Freundlich Isotherm Model Constants.....	4-15
Table 2 Second Order Potential Driving Kinetic Model Constants.....	4-16
Table 3 Thomas Model Constants	4-17
Table 4 Breakthrough and Exhaustion Capacity for Phosphorus Adsorption	4-18
Table 5 Summary of Media Capacity	4-19

List of Figures

Figure 1 Schematic experimental configuration of TDP adsorption kinetics on adsorbent media	4-20
Figure 2 Schematic experimental configuration of TDP adsorption breakthrough on adsorbent media	4-20
Figure 3 Phosphorus equilibrium isotherm for AO _{CMc} (0.85 - 2 mm).....	4-21
Figure 4 Phosphorus equilibrium isotherm for AO _{CMc} (2 – 4.75 mm)	4-21
Figure 5 Phosphorus equilibrium isotherm for AO _{CMp} (2 – 4.75 mm).....	4-22
Figure 6 Phosphorus equilibrium isotherm for Expanded clay substrate (0.85 – 2 mm)	4-22
Figure 7 Phosphorus equilibrium isotherm for Expanded clay substrate (2 – 4.75 mm)	4-23
Figure 8 Phosphorus equilibrium isotherm for Pumice substrate (2 – 4.75 mm).....	4-23
Figure 9 Phosphorus equilibrium isotherm for Bioretention soil media (0.001 – 10 mm).....	4-24
Figure 10 Phosphorus equilibrium isotherm for UCF-1 (0.5 – 4.75 mm)	4-24
Figure 11 Phosphorus equilibrium isotherm for UCF-2 (0.85 – 10 mm)	4-25
Figure 12 Phosphorus equilibrium isotherm for Expanded Shale-1 (2 – 10 mm)	4-25
Figure 13 Phosphorus equilibrium isotherm for Expanded Shale-2 (0.45 – 4.5 mm)	4-26
Figure 14 Phosphorus equilibrium isotherm for AO _{CMpcc} and CM _{pcc} (0.85 – 2 mm).....	4-26
Figure 15 Phosphorus adsorption kinetics for AO _{CMc} (0.85 - 2 mm)	4-27
Figure 16 Phosphorus adsorption kinetics for AO _{CMc} (2 – 4.75 mm)	4-27
Figure 17 Phosphorus adsorption kinetics for AO _{CMp} (2 – 4.75 mm)	4-28
Figure 18 Phosphorus adsorption kinetics for Expanded clay substrate (0.85 – 2 mm).....	4-28
Figure 19 Phosphorus adsorption kinetics for Expanded clay substrate (2 – 4.75 mm).....	4-29
Figure 20 Phosphorus adsorption kinetics for Pumice substrate (2 – 4.75 mm)	4-29
Figure 21 Phosphorus adsorption kinetics for Bioretention soil media (0.001 – 10 mm)	4-30
Figure 22 Phosphorus adsorption kinetics for UCF-1 (0.5 – 4.75 mm)	4-30
Figure 23 Phosphorus adsorption kinetics for UCF-2 (0.85 – 10 mm)	4-31
Figure 24 Phosphorus adsorption kinetics for Expanded Shale -1 (2 - 10 mm)	4-31
Figure 25 Phosphorus adsorption kinetics for Expanded Shale - 2 (0.45 – 4.5 mm)	4-32
Figure 26 Phosphorus adsorption kinetics for AO _{CMpcc} and CM _{pcc} (0.85 – 2 mm)	4-32
Figure 27 Phosphorus breakthrough test for AO _{CMc} (0.85 – 2 mm)	4-33
Figure 28 Phosphorus breakthrough test for AO _{CMc} (2 – 4.75 mm)	4-33
Figure 29 Phosphorus breakthrough test for AO _{CMp} (2 – 4.75 mm)	4-34
Figure 30 Phosphorus breakthrough test for Pumice substrate (2 – 4.75 mm).....	4-34
Figure 31 Phosphorus breakthrough test for Bioretention soil media(0.001 – 10 mm)	4-35

Figure 32 Phosphorus breakthrough test for UCF-1 (0.5 – 4.75 mm).....	4-35
Figure 33 Phosphorus breakthrough test for UCF-2 (0.85 – 10 mm).....	4-36
Figure 34 Phosphorus breakthrough test for Expanded Shale-1 (2 – 10 mm).....	4-36
Figure 35 Phosphorus breakthrough test for Expanded Shale - 2 (0.45 – 4.5 mm).....	4-37
Figure 36 Phosphorus breakthrough test for AOCM _{pcc} and CM _{pcc} (0.85 – 2 mm).....	4-37
Figure 37 Phosphorus Adsorption-Desorption test for UCF-1 media (0.5 – 4.75 mm). The distance and area between the data and the C/C_0 line = 1.0 represents phosphorus desorption in terms of concentration and mass, respectively.	4-38
Figure 38 Phosphorus Adsorption-Desorption test for UCF-2 (0.85 – 10 mm). The distance and area between the data and the C/C_0 line = 1.0 represents phosphorus desorption in terms of concentration and mass, respectively.	4-38
Figure 39 Phosphorus Adsorption-Desorption test for Expanded Shale -1 (2 - 10 mm). The distance and area between the data and the C/C_0 line = 1.0 represents phosphorus desorption in terms of concentration and mass, respectively.	4-39
Figure 40 Phosphorus Adsorption-Desorption test for Expanded Shale -2 (0.45 – 4.5 mm). The distance and area between the data and the C/C_0 line = 1.0 represents phosphorus desorption in terms of concentration and mass, respectively.	4-39
Figure 41 Phosphorus Adsorption test for AOCM _c (2 – 4.75 mm). This media did not exhibit any desorption and all data are below the C/C_0 line = 1.0; therefore the distance and area between the data and the C/C_0 line = 1.0 represents phosphorus adsorption in terms of concentration and mass, respectively.	4-40

INTRODUCTION

Phosphorus is recognized as a primary nutrient discharged in excess to surface waters and ground water; and such enrichment by phosphorus is regarded as a main reason for eutrophication. The aesthetic, chemical and ecological degradation of receiving waters as a result of rainfall-runoff discharges enriched with phosphorus (nitrogen notwithstanding) has led to significant public stakeholder concerns and regulation intended to mitigate the significant environmental and ecological impacts (Bowes et al. 2005). Nutrients are generated from nonpoint (diffuse) biogenic and anthropogenic sources such as vegetation, fertilizers, detergents, animal waste, infrastructure, and traffic; as well as point sources such as domestic and industrial sewage waters, and transferred into natural and built environs through many different pathways (Ray 1997; Waschbusch et al. 1999). The built environs as the impervious interface that transforms rainfall to runoff, is a major nonpoint source and pathway of nutrients. Runoff can contain high phosphorus concentrations that can accelerate eutrophication for many receiving waters (USEPA 1993; Dean et al. 2005; Kim et al. 2008). There has been much work in Europe and North America to reduce nutrient point sources from industrial and municipal sewage, but nonpoint source control of urban rainfall-runoff, is still of major concern and nonpoint sources are more difficult to manage than wastewater (Duda, 1993; Sansalone 2005).

As a stormwater pollutant load, many methods of controlling phosphorus have been investigated, such as constructed wetland system (Gervin and Brix 2001; Seo et al. 2005), filtration, infiltration and detention/retention basins (Bartone and Uchirin 1999; Dechesne et al. 2005; Hsieh et al. 2007), in-situ filtration (Sansalone and Teng 2004, Teng and Sansalone 2004), storm-treat systems (sedimentation tank) (Sonstrom et al. 2002), urban wet detention ponds (Wu et al. 1996; Comings et al. 2000; Wang et al. 2004), and vegetative controls (Barrett et al. 1998). Whether identified, explicitly or not, the basic mechanisms in these studies are sedimentation and filtration of particulate matter (PM) with the potential of adsorption either during or prior to sedimentation or filtration. Other studies explicitly demonstrated the role of adsorption during the filtration process onto oxide-coated media (Sansalone and Teng 2004). While sedimentation occurs in all unit operations, whether by design or otherwise, designs based strictly on sedimentation such as with detention/retention basins, tanks or even hydrodynamic separators, designed based on surface overflow rate concepts are challenged in populated urban area since there is generally a requirement of large operational area and volume, if suspended PM and the associated phosphorus requires separation. Additionally, sedimentation is a physical mechanism intended to separate PM, not soluble phosphorus, unless there is partitioning from solution to PM during sedimentation. However, while partitioning does occur in the sedimentation process, there is also the potential for re-partitioning back to the water column due to changing water chemistry conditions during runoff storage. While shallow basins with large surface areas can have significant gas transfer with the atmosphere, thereby remaining oxic, below-grade systems such as tanks, tunnels, and storage pipelines do not allow such exchange, with anoxic/anaerobic conditions that can occur within 48 hours. Another very real challenge for these basins is the potential of contaminating underlying soil and groundwater, whether with phosphorus species, metals more mobile nitrogen species such as nitrate. The potential for groundwater and natural spring contamination in karst areas such as central and north Florida is well-recognized and significant (Arias et al. 2006). Furthermore, beyond Florida, the direct or proximate communication between runoff stored in an unlined basin and groundwater or in karst conditions,

is common in nearly 25% of the United States. Despite these challenges, if such basins or tanks are properly designed, operated, and frequently maintained (a rare occurrence) such systems can be effective for the temporary separation of phosphorus as well as the long-term management of runoff PM sludge containing phosphorus and other constituents that partition during the sedimentation and storage phase. Ignoring the potential for phosphorus separation, uptake and burial, the importance of above-ground basins, when properly designed, operated and maintained, is the ability to provide some degree of hydrologic restoration through infiltration, evaporation and storage. However, given the difficulty of such basins to capture high levels of soluble phosphorus, the potential of phosphorus leaching as vegetation dies, the potential of phosphorus migration to karst areas, and generally large basin surface area requirements for separation of suspended PM exist; requires adsorptive-filtration as secondary treatment.

More recently manufactured filtration-type unit operations are becoming more widely used in urban conditions because of their smaller footprint and their ability to separate suspended PM albeit at lower surface loading rate. For a filter the surface loading rate is based on the “representative” filter surface area, depending on the direction of flow. For example for an axial prismatic filter, the surface area is the cross-sectional area which is orthogonal to flow. For a radial cartridge filter with inward radial flow the two-dimensional flow is radial (ignoring the parabolic curvature in the third dimension) and therefore the surface area is the representative radial surface (at the geometric mean radius). A major consideration for filtration systems, even stormwater media systems intended to function with adsorption as a primary mechanism is clogging (excessive head loss with filter ripening). This is of particular concern for passive filters, driven primarily by head differences and gravity. While mechanisms such as filter ripening can be beneficial for adsorptive-filtration performance; progressive filter ripening results in increasingly non-linear head loss and eventual clogging for the filter.

Filtration systems (engineered filters, bioretention, infiltration trenches) that are not properly designed or maintained commonly result in premature clogging. Much of this premature failure can be tied to a lack of understanding of filtration mechanisms for urban rainfall-runoff or snowmelt loadings, the lack of upstream primary treatment that lowers primary effluent PM levels to the range of 20 to 50 mg/L (Cristina and Sansalone 2003) with sustainable filters loaded by an influent less than 20 to 30 mg/L without regular on-line backwashing; or simply improper filter and upstream unit operation design. An adsorptive-filter will fail (clogging, or poor adsorption and/or filtration) without proper stormwater conditioning by a primary unit operation or the wrong media selection, such as sand or perlite. Five decades of unit operation and process knowledge gained from the wastewater and drinking water industries should be kept in mind when designing and maintaining stormwater filters; including the benefits of flow equalization. It is noted that adsorptive-filtration is a secondary-tertiary unit operation and as such requires upstream conditioning. Additionally, there are a plethora of media that are promoted in the marketplace may be well-intentioned from either a business point of view or from an intuitive point of view, but simply cannot achieve effective phosphorus or metals removal efficiency (Bubba et al. 2003; Liu et al. 2005; Kim et al. 2008). To meet current and expected stormwater chemistry treatment requirement, advanced in-situ phosphorus treatment technologies and amendment materials have to be developed for urban rainfall-runoff. These technologies represent a combination of engineered media, an engineered system, and quantitative operation and maintenance (O&M) practices that synthesizes influent chemistry and loadings, effluent

requirements and the quantitative behavior of the engineered media and system. This chapter focuses on the engineered media component of such unit operations/processes.

Many filtration media types were developed with certain purposes. For example, manganese oxide media, including manganese coated polymeric media (MOPM) and manganese oxide coated cementitious media (MOCM) were evaluated by Liu and Sansalone (2004a, 2004b, 2005a, 2005b) in sorptive filtration system as a rainfall-runoff or snowmelt unit operation and process media for treatment metal species. Birnessite-coated and cryptomelane-coated forms of manganese, as well as iron oxide coated media were tested by Liu et al. (2001a, 2001b), Sansalone (1999a, 1999b), Li et al. (1999). Sansalone and Buchberger (1995) utilized filtration and exfiltration systems for treatment of metals in runoff that included iron oxide coated media under aerobic conditions. Results indicate a significant capacity for metal species by such media, with the surface chemistry favoring the adsorption of metal species with selected oxides of iron favorable to phosphorus. Also it was from these studies that specific form of oxide, specific surface area and surface charge were found to be critical relative to performance capability.

In order to remove phosphorus in rainfall-runoff, as well as receiving water bodies, aluminum oxide, iron oxide, or a combination of these oxides are utilized (Kim et al. 2008; Liu et al. 2005). In particular, aluminum oxide can be used in combination with porous, high surface area substrate or calcium-containing substrate such as concrete to produce an effective adsorptive media. While plain concrete media is temporarily effective, the mass transfer is that of precipitation resulting in an unstable build up of phosphorus on the media surface with such physical precipitate build-up being sloughed off periodically into the effluent. This result was also observed for metal precipitates on concrete media (Liu et al. 2005).

To date very few quantitative tools evaluating adsorptive-filter media for phosphorus adsorption have been implemented. Additionally continues to be limited information available and divergent performance claims for phosphorus removal for both manufactured and natural filtration systems using un-quantified media. Media applications that do exist with reported information tend to experience high performance variability (Davis et al. 2006, Heieh et al. 2007) or result in exporting phosphorus, or leaching of other indices such as metals or pH. Again, these challenges are due to the limited quantitative information of the behavior of the filter material. Moreover, availability and rapid replacement costs are concerns when media of lower capacity or longevity is employed for commercial use. Some materials have abundant sources and relative low cost, such as sand, peat, perlite or organic based materials made from different types of waste, but their performance for phosphorus removal does not satisfy the requirements imposed by regulatory agencies or public communities or meet TMDLs under many conditions.

The purpose of this study is to quantitatively examine the phosphorus removal performance of filter media. These filter media were examined based on standard engineering methods of adsorption phenomena and requirements of adsorption behavior for media. These requirements include a quantitative description of:

- (1) equilibrium isotherms (how much phosphorus can media uptake),
- (2) kinetics (how rapidly can phosphorus be taken up by the media), and
- (3) breakthrough (under flow-through hydraulic loading rates, what is the removal level and how long does the media lasts before performance diminishes, i.e. maintenance frequency).

Successful deployment of any media system requires the comparison of media behavior on a rigorous and equal basis through these three quantitative descriptions; in addition to desorption or leaching quantification. With such a methodology, media comparisons are clearly illustrated as a series of equilibria, kinetics and breakthrough results; providing a much-needed rigorous and defensible basis for to predict media performance.

MATERIALS AND METHODOLOGY

Engineered Soil Media Preparation

Materials:

Clay, a blowing agent and water are necessary materials that were used for raw substrate preparation. Aluminum nitrate was used for media coating.

Methodology:

Raw clay substrate

Dry clay was measured in appropriate quantities and well mixed with water using a drill mixer. The mixture is allowed to stand for a short while to generate enough pores. The well developed mixture with pores due to the effect of blowing agent was then transferred to an electric kiln. The mixture is fired in the kiln at a predetermined heating procedure.

By firing the mixture in the kiln, all the moisture is evaporated and a dry raw substrate with a large number of pores is obtained. This raw substrate is crushed to finer particles using an crusher (400 lb/hour). The soil media so obtained after crushing is passed through a series of sieves. Four particle size gradations namely particles > 4.75 mm, $2 \sim 4.75$ mm, $0.85 \sim 2$ mm, and < 0.85 mm were obtained using the appropriate size sieves. The soil media size selection was based on the filtration parameters such as adsorption capability, hydraulic conductivity and head loss ($2 \sim 4.75$ mm and $0.85 \sim 2$ mm).

Coating

$\text{Al}(\text{NO}_3)_3 \cdot 9\text{H}_2\text{O}$ was used to prepare the coating solution. 1 M Al salt solution was mixed with washed dry media substrate in batch, until the substrate was just submerged and heated to dryness at 105°C or higher. After cooling the media is rinsed to a pH range of 5. The final media (AOCM_c) is ready to use.

Engineered Soil Media Tests

Materials:

Phosphorus solution

A phosphorus stock solution was prepared by dissolving anhydrous potassium dihydrogen orthophosphate (KH_2PO_4) powder (Analytical reagent grade, Fisher Scientific) into de-ionized (D.I.) water. The stock solutions were calibrated to 100.00 mg/L and 1000.00 mg/L concentrations and then utilized for standard solutions with DI water as necessary.

Media as Adsorbents

A wide range of candidate media were selected and tested in this study. The major composition and size of the adsorbents were summarized in Table 1. Three different aluminum oxide-coated media (AOCM) were prepared and examined, with soil-based clay media (AOCM_c), pumice (AOCM_p) and concrete (AOCM_{pcc}) as the raw substrate materials, respectively. The corresponding uncoated substrates of these media were also tested as controls.

The adsorbents include:

1. AOCM_c (0.85 – 2 mm) (aluminum oxide coated clay media)
2. AOCM_c (2 – 4.75 mm) (aluminum oxide coated clay media)
3. Expanded clay substrate (0.85 – 2 mm) (clay substrate only of AOCM)
4. Expanded clay substrate (2 – 4.75 mm) (clay substrate only of AOCM)
5. AOCM_p (2 – 4.75 mm) (aluminum oxide coated pumice media)
6. Pumice substrate (2 – 4.75 mm) (pumice substrate only)
7. AOCM_{pcc} (0.85-2 mm) (aluminum oxide coated concrete media)
8. Concrete substrate (0.85 – 2 mm) (concrete substrate only)
9. Bioretention soil media (1m – 10 mm) (commercial mixture for Prince George's County, Maryland P-index = 25)
10. UCF - 1 (0.5 – 4.75 mm) (proprietary mix including tire crumbs)
11. UCF -2 (0.85 – 10 mm) (supplied by UCF through FDEP request)
(proprietary mix including tire crumbs)
12. Expanded shale - 1 (2 – 10 mm) (supplied by UCF through FDEP request)
(commercial expanded shale)
13. Expanded shale -2 (0.45 – 4.5 mm) (commercial expanded shale)

Methodology:

The total dissolved phosphate (TDP) adsorption characterization experiments consist of an adsorption equilibrium study, an adsorption kinetic study, a one-dimensional column breakthrough study and a desorption study. Phosphorus was measured by a HACH DR/5000 Spectrophotometer using PhosVer 3 Ascorbic Acid Method (Standard Method 1998). The ascorbic acid method was used to detect orthophosphate and a persulfate digestion was used to convert any other forms of phosphorus to orthophosphate. The amount of adsorbate that was adsorbed on the adsorbent was then calculated from the difference between the initial and equilibrium solute concentrations. A multi-meter (Orion 290A combination electrode) was

calibrated using a 3-point calibration curve with reference units at a pH of 4, 7, and 10. All measurements were duplicated and repeatability was assured with experimental error at $\pm 5\%$.

Adsorption Equilibrium (Isotherm) Study

In order to estimate static or dynamic adsorption capacity, it is essential to have information on adsorption equilibrium to begin to quantify how much phosphorous can be adsorbed (equilibrium capacity). A common way to represent the adsorption equilibrium is the isotherm from which the amount of phosphorus species adsorbed under a given set of chemistry conditions can be determined for a given media. In the present study, the specific working phosphorus concentration utilized to obtain isotherm data are: 0, 0.05, 0.5, 1.0, 2.5, 10, 25 and 50 mg/L. It is noted that a single point measurement is not an isotherm. Just as a single sample cannot represent the characteristics of a runoff event; a single point measurement cannot represent the equilibrium capacity except at that specific point. Ionic strength was fixed at 0.01 M using KCl. Solution pH was adjusted and maintained at 7.0 throughout experiments by dropwise addition of HCl or NaOH. 0.5 g adsorbent and 40 ml of phosphate solution were added in a 50 ml polyethylene centrifuge tube. The mixture was mixed on a horizontal bench shaker at a rate of 100 rpm allowing adsorption to take place at 20°C until equilibrium reached, usually 24 hr. The content in the centrifuge tube was then filtered through 0.45 μm syringe filter and the total dissolved phosphate concentration in the filtrate was measured using a spectrophotometer (HACH, DR5000). The amount of adsorbate that was adsorbed on the adsorbent was then calculated from the difference between the initial and equilibrium solute concentrations.

Adsorption Kinetic Study

To determine how rapidly a media will adsorb phosphorous, the kinetics of adsorption were investigated in the recirculating flow-through reactor. The sorbent solution ratio was 2 L to 20 g of media. The ionic strength was set at 0.01 M as KCl. The pH was maintained at 7. The surface loading rate was kept as 40 L/min-m² throughout the experiment. The surface loading rate was chosen based on real-time range of rainfall-runoff surface loading. For example, in Sansalone and Buchberger (1997)'s study, a surface loading rate of 50 L/min-m² is utilized for the peak of 1-year return event at an experimental site treating overland flow. Usually, the surface loading rate should range within 20 to 60 L/min-m². While the return event is a dated concept, it has heuristic value as a design yardstick. In this study, a representative value of 40 L/min-m² was maintained. Duplicate samples of 10 mL were collected at predetermined time intervals from the sampling port. The sample solution was then filtered through 0.45 μm filter and total dissolved phosphate concentration was determined using a spectrophotometer (HACH, DR5000). The experimental set-up of kinetic study is shown in Fig. 1.

Column Breakthrough Study

The column breakthrough study is a performance indicator (i.e. media bed service life), which is based on a predetermined level of performance (effluent concentration). Breakthrough is critical for prediction of how the media will perform and how frequently it needs to be replaced or maintained to ensure the desired performance is achieved. Breakthrough occurs when the predetermined removal performance is no longer achievable as a result of diminished

adsorption capacity (or effluent concentration). Breakthrough is quantified either on the number of pore volumes (PV) (volume of fluid equivalent to the hydraulically-available pore space of the media system); or the number of bed volumes (media plus pore volume). A Bed Volume (BV) of solution is equal to the volume of absorbent media and macroscopic pore volume contained in the media that are utilized, hence the media performance is measured based on the number of Bed Volumes (N_{BV}) that flow through the media system, in these tests a prismatic axial column.

Phosphorus adsorption for different adsorbents under continuous flow-through loading was investigated using a Teflon PFA column. A known mass of dry media was packed inside the column to absorb the phosphorus from the flow-through solution. Influent P concentration (C_0) was set up as 0.5 mg/L. The constant influent feed to the column is supplied by a peristaltic pump. The influent pH was adjusted to 7.0 and controlled throughout the experiment. Samples were collected at regular time intervals and effluent TDP (total dissolved phosphate) concentration (C_e) was then determined. The column studies were terminated when the media reached exhaustion (V_{exh}) i.e. C_e/C_0 equal to 0.9 (10% removal rate). The experimental set-up of column breakthrough study is shown in Fig. 2.

Modeling

In order to quantitatively evaluate the media performance, optimize the design of sorption systems, and explain the physical-chemical phenomena it is necessary to establish an appropriate mathematical model to describe the experimental data. Often mechanistic or statistical explanations are ignored in media evaluations.

The amount of adsorption at equilibrium, q_e [mg/g], was computed as follows:

$$q_e = \frac{(C_0 - C_e)V}{W} \quad (1)$$

C_0 and C_e are the initial and equilibrium solution concentrations [mg/L], respectively; V the volume of the solution [L] and W the weight of adsorbent used [g].

Adsorption Isotherm Modeling

Isotherm equations can represent the experimental data (equilibrium capacity) in a concise manner and such equations can also be used to predict behavior under conditions that have not been investigated. An isotherm model that has been commonly utilized to model clays and other heterogeneous media surfaces is the Freundlich isotherm. The Freundlich isotherm is often used for media with heterogeneous surfaces and surface affinities.

$$q = K_F C^n \quad (2)$$

K_F is the Freundlich constant and n the Freundlich exponent and the reciprocal is indicative of adsorption intensity and C_e the concentration of adsorbate in solution at equilibrium [mg/L]. The experimental data were fit to the Freundlich model using non-linear regression analysis.

The Freundlich expression has the form of a power law expression and was initially regarded as a completely empirical isotherm. However, for a mono-component system, the Freundlich isotherm can be obtained theoretically when an exponential distribution of adsorption energy is assumed. Alternatively, isotherm equations could also be developed from theory, based on kinetics for the interactions with the media surface, dissolved species and surface-complexed species.

Adsorption Kinetic Modeling

The study of adsorption kinetics describes the solute uptake rate, which evidently controls the residence time of adsorbate uptake at the solid-solution interface. Here, the kinetics of phosphorus adsorption on the media was analyzed using a transformation of second-order potential driving kinetic model developed by Liu et al (2005). The conformity between experimental data and model predicted values was evaluated by coefficients of determination (R^2), although a variety of statistical test results can be examined.

The differential equation:

$$\frac{dq_t}{dt} = k(q_e - q_t)^2 \quad (3)$$

Integrating Eq. (3) and applying the boundary conditions, gives:

$$\frac{1}{(q_e - q_t)} = \frac{1}{q_e} + kt \quad (4)$$

Eq. (4) can be rearranged to obtain the expression for q_t :

$$q_t = \frac{q_e t}{\frac{1}{q_e k} + t} \quad (5)$$

k is the equilibrium rate constant of pseudo second-order adsorption [g/mg-min].

Breakthrough Studies Modeling

The adsorption data from column studies was analyzed using the Thomas model as follows:

$$\frac{C_e}{C_0} = \frac{1}{1 + \exp\left[\frac{K_T(q_0 m - C_0 V)}{Q}\right]} \quad (6)$$

C_e is the effluent adsorbate concentration [mg/L], C_0 the influent adsorbate concentration [mg/L], K_T the Thomas rate constant [L/min-mg], q_0 the maximum solid phase concentration of

the solute [mg/g], m the mass of the adsorbent [g], V the throughput volume [L], and Q is the volumetric flow rate [L/min].

RESULTS AND DISCUSSION

Adsorption Equilibrium Isotherm Study

These results detail the summary provided in a quarterly report on media. Adsorption isotherms express the variation of specific adsorption with equilibrium concentrations of adsorbate in bulk solutions at constant temperature (Liu et al 2005). Several relationships can be used to describe the experimental data. Freundlich isotherm has a theoretical assumption of heterogeneous surface properties and was utilized to simulate the data obtained from the isotherm experiments, given the heterogeneous surface properties of the different adsorbents. Table 1 summarizes the Freundlich model constants and correlation determination R^2 of the fitness. Fig. 3 through Fig. 12 depict the adsorption isotherm for phosphorus on the media respectively, as well as the theoretical Freundlich equations. In all the cases, R^2 is no less than 0.94. In the Freundlich isotherm equation, the coefficient K_F is an indication of adsorption capacity and n reflects the steepness of the curve. From Table 1, it can be found that AOCC_c (0.85 – 2 mm) had an adsorption capacity of 3.63 mg/g, followed by AOCC_{pcc} (1.32 [mg/g]) and AOCC_c (2 – 4.75 mm, 1.05 [mg/g]), respectively. Generally, oxide coated media had significantly higher adsorption capacities than all the other media or media substrates. It was observed that the phosphate adsorption capacity of the clays be related to both the alumina – silica molecular ratio of the clay minerals and the alumina content of clay media. For example, a basic adsorption reaction of phosphorus with AOCC_c is the chemical adsorption reactions between phosphorus ions in solution and alumina surface groups on the clay. The significance of such reaction was also verified by the free energy calculations for the adsorption of phosphate on Al_2O_3 .

In addition, it can be found that adsorption capacity of different adsorbents can vary from 3.63 mg/g (AOCC_c) to a very low value of 0.0009 mg/g (UCF – 2). The more than 4000 times difference further demonstrates the diverse performance of the media being deployed and the necessity of quantitatively examination and comparison of different adsorbents. Results illustrate that the aluminum-coated clay media significantly outperformed all other media with respect to the highest equilibrium capacity.

Adsorption Equilibrium Kinetic Study

Fig. 13 through Fig. 22 illustrates the results obtained by kinetics experiments for the adsorption kinetics of phosphorus onto different adsorbents. A second order potential driving kinetic model was used to simulate the behavior (Liu et al 2005). As with the isotherm results, the time profiles of phosphorus uptake for the aluminum oxide and iron oxide media are similar: a single, smooth and continuous curve leading to saturation, with significantly higher rates of adsorption than all other media. The smooth and continuous curvatures may be an indication of the possible monolayer coverage of phosphorus on the surface of the adsorbents. A lumped analysis of kinetic data is sufficient for adsorption system design purpose and the simplicity of

the mathematical equation makes it convenient for practical use. The fit of the model is examined using a coefficient of determination.

The kinetic study results in the figures and in Table 2 are consistent with results of adsorption isotherm. The coated media illustrates much shorter equilibrium time and higher removal efficiency. For instance, q_e is 0.096 mg/g and 0.013 mg/g for AO_{CMc} (0.85 – 2 mm) and AO_{CMc} substrate (0.85 -2 mm), respectively. The only difference between the two adsorbents is the aluminum oxide coating, while the q_e of the coated one is more than 7 times higher than that of the corresponding raw substrate. This result clearly reinforces the effectiveness of aluminum oxide coating for the improvement of media substrate adsorption capacity.

In addition, the data of UCF – 1 and UCF – 2 media cannot be fit with a potential driving kinetics model since negative q_e was obtained from the experiments, resulting from the phosphorus actually being desorbed from the UCF adsorbents.

Breakthrough Study

For one-dimensional column studies, the total dissolved phosphorus (TDP) concentration tested was 0.5 mg/L and the pH of the feed solution was 7.0. The mass of media used in the tests were determined by a comprehensive consideration of media capacity, L/D ratio of the reactor, time scale of experiments and experimental set-up configuration as well. Fig. 23 through Fig. 32 plots the ratio of effluent to influent phosphate concentration versus the flow through the column (expressed as number of bed volume, N_{BV})., the breakthrough curve cannot be obtained for all of the media tested due to poor behavior of the low capacity media. For bioretention soil media, the experiment run were difficult due to erosion of the clayey and fine silty fraction of the media. Breakthrough results are summarized in Table 3 and 4.

Again, uncoated media exhibit poor adsorption capacity and the performance of the UCF and expanded shale had even lower capacity. C_e/C_0 ratio is larger than 1, indicating that on the contrary of removing phosphorus from solution, these media release, or export phosphorus themselves. For the media showing good phosphorus removal capacity, the breakthrough was reached ($C_e/C_0 = 0.1$) from almost immediately to about 600 N_{BV} (AO_{CMc} (0.85 – 2 mm)). However, several media exhibited very high exhaustion capacity: 1000 N_{BV} for AO_{CM_{pcc}} and CM_{pcc} and 2500 N_{BV} for AO_{CM_p}, respectively. Moreover, a small break on the breakthrough curve may be observed for some media, which could be resulted from the instability when the media capacity was reached or slight desorption of phosphorus.

As a result of the isotherm, kinetics and breakthrough results, field deployment of clay-based AO_{CM} was chosen. Field testing is described in later chapters. An equally viable choice would be concrete-based AO_{CM} once the recycled or crushed concrete was carbonated.

Desorption Study

Breakthrough curves as well as desorption experimental data for the tested media are shown in Figures 33 to 37. It can be observed that for UCF and ESF media breakthrough is reached within 20 bed volumes. Moreover, all the four media exhibit certain degree of P leaching during

the breakthrough experiment which was exemplified as a higher effluent concentration compared with the initial P concentration. In such conditions, new adsorbent with the same mass was loaded into the reactor after BTC tests to evaluate desorption or leaching behavior of the media. Both UCF and ESF media release P. By comparison, AOCM showed much better performance without any desorption. With respect to all categories of media behavior, the clay-based soil media outperformed all other media tested and was chosen for field testing.

REFERENCES

- Arias M., Da Silva-Carballal J., Garcia-Rio L., Mejuto J., Nuñez A. (2006). "Retention of phosphorus by iron and aluminum-oxide-coated quartz particles." *J. of Colloid and Interface Sci.*, 295, 65-70.
- Barrett, M. E., Walsh, P. M., Malina, J. F., and Charbeneau, R. J. (1998). "Performance of Vegetative Controls for Treating Highway Runoff." *J. Environ. Eng.*, 124(11), 1121-1128.
- Bartone, D. M., and Uchrin, C. G. (1999). "Comparison of Pollutant Removal Efficiency for Two Residential Storm Water Basins." *J. Environ. Eng.*, 125(7), 674-677.
- Braja M. D. (2001) "Principles of Geotechnical Engineering" 5th edition, Thomson Learning
- Bowes, M.J., House, W.A., Hadgkinson, R.A. and Leach, D.V., 2005. Phosphorus-Discharge Hysteresis During Storm Events Along a Rivers Catchment: the River Swale, UK. *Water Res.*, 29, 751-762.
- Bubba, M. D., Arias, C. A., and Brix, H. (2003). "Phosphorus Adsorption Maximum of Sands for Use as Media in Subsurface Flow Constructed Reed Beds as Measured by the Langmuir Isotherm." *Water Res.*, 37, 3390-3400.
- Comings, K. J., Booth, D. B., and Horner, R. R. (2000). "Storm Water Pollutant Removal by Two Wet Ponds in Bellevue, Washington." *J. Environ. Eng.*, 126(4), 321-330.
- Cristina C. and Sansalone J.J., (2003). "First Flush, Power Law and Particle Separation Diagrams For Urban Storm-Water Suspended Particulates", *J. of Environmental Engineering*, 129 (4), 298-307.
- Davis A. P., Shokouhian M., Sharma H. and Minami C. (2006). "Water Quality Improvement through Bioretention Media: Nitrogen and Phosphorus Removal", *Water Environ. Res.*, 78 (3), 284 - 293
- Dean, C.M., Sansalone, J.J., Cartledge, F.K., Pardue, J.H., 2005. Influence of hydrology on rainfall-runoff metal element speciation. *Journal of Environmental Engineering-ASCE* 131(4), 632-642.
- Dechesne, M., Barraud, S., and Bardin, J. P. (2005). "Experimental Assessment of

Stormwater Infiltration Basin Evolution.” *J. Environ. Eng.*, 131 (7), 1090-1098.

Duda A.M., 1993. Addressing nonpoint sources of water pollution must become an international priority. *Water Sci. Technol.*, 28, 1-11.

Hsieh C. H., Davis A. P. and Needelman B. A. (2007). “Bioretention Column Studies of Phosphorus Removal from Urban Stormwater runoff” *Water Environ. Res.*, 79 (2), 177 - 184

Gervin, L., and Brix, H. (2001). “Removal of Nutrients from Combined Sewer Overflows and Lake Water in a Vertical-Flow Constructed Wetland System.” *Water Sci. Technol.*, 44(11-12), 171-176.

Kim J-Y., Ma J., Howerter K., Garofalo G., and Sansalone J.J., “Interactions Of Phosphorus With Anthropogenic And Engineered Particulate Matter As A Function Of Mass, Number And Surface Area”, *Urban Water Systems, Monograph 11*, Edited by James W. CHI Publications, Guelph, Ontario, 20 pp. Feb. 2008

Li Y, Buchberger S. G., and Sansalone J. J. (1999). “ Variable Saturated Flow in A Storm Water Partial Exfiltration Trench.” *J. Environ. Eng.*, 125 (6), 556-565

Liu D., Sansalone J. J. and Cartledge F. K. (2005). “Adsorption Kinetics for Urban Rainfall-Runoff Metals by Composite Oxide-Coated Polymeric Media.” *J. Environ. Eng.*, 131 (8), 1168-1177

Liu D., Sansalone J. J. and Cartledge F. K. (2005). “Comparison of Sorptive Filter Media for Treatment of Metals in Runoff.” *J. Environ. Eng.*, 131 (8), 1155-1167

Liu D., Sansalone J. J. and Cartledge F. K. (2004). “Adsorption Characteristics of Oxide Coated Polymeric Media ($\rho_s < 1.0$) for Stormwater Treatment: Batch Equilibria and Kinetics.” *J. Environ. Eng.*, 130 (4), 374-382

Liu D., Sansalone J. J. and Cartledge F. K. (2004). “Adsorption Characteristics of Oxide Coated Polymeric Media ($\rho_s < 1.0$) for Storm Water Treatment: Equilibria and Kinetics Models.” *J. Environ. Eng.*, 130 (4), 383-391

Liu D., Teng Z. Sansalone J. J. and Cartledge F. K. (2001). “Surface Characteristics of Sorptive-Filtration Storm Water Media: Low Specific Gravity ($\rho_s < 1.0$) Oxide Coated Floating Media.” *J. Environ. Eng.*, 127 (10), 868-878

Liu D., Teng Z., Sansalone J. J. and Cartledge F. K. (2001). “Surface Characteristics of Sorptive-Filtration Storm Water Media: Higher Specific Gravity ($\rho_s > 1.0$) Oxide Coated Fixed Media.” *J. Environ. Eng.*, 127 (10), 879-888

Ray, H. (1997). “Street dirt as a phosphorus source in urban stormwater.” *Ph.D. dissertation*, University of Alabama at Birmingham, 125.

Sansalone J. J. (1999). "Adsorptive-Infiltration of Metals in Urban Drainage-Media Characteristics." *Sci, Tot. Environ.*, 235 (1-3), 179-188

Sansalone J. J. (1999). "In-situ Performance of a Passive Treatment System for Metal Elements in Urban Surface Waters." *Wat. Sci. Tech.*, 39 (2), 193-200

Sansalone J. J. and Buchberger S. G. (1995). "An Infiltration Device as a Best Management Practice for Pollutants in Highway Runoff." *Wat. Sci. Tech.*, 32 (1), 119-125

Sansalone J. J., Koran J., Buchberger S. G. and Smithson J. (1998). "Physical Characteristics of Highway Solids Transported During Rainfall." *J. Environ. Eng.*, 124 (5), 427-440

Sansalone, J.J., and Teng, Z. (2005). "Transient Rainfall-Runoff Loadings to a Partial Exfiltration System: Implications for Urban Water Quantity and Quality." *J. Environ. Eng.*, 130(9), 990-1007.

Sansalone J.J. (2005), "Perspective On The Synthesis Of Unit Operations And Process (UOP) Concepts With Hydrologic Controls For Rainfall-Runoff", *J. of Environmental Engineering*, 131 (7): 995-997.

Seo, D. C., Cho, J. S., Lee, H. J., and Heo, J. S. (2005). "Phosphorus Retention Capacity of Filter Media for Estimating the Longevity of Constructed Wetland." *Water Res.*, 39(11), 2445-2457.

Sonstrom, R. S., Clausen, J. C., and Askew, D. R. (2002). "Treatment of Parking Lot Stormwater Using a StormTreat System." *Environ. Sci. Technol.*, 36(20), 4441-4446.

Teng, Z., and Sansalone, J.J. (2004). "In situ partial exfiltration of rainfall runoff. II: particle separation." *J. Environ. Eng.*, 130(9), 1008-1020.

U.S. Environmental Protection Agency (1993). "Handbook: Urban Runoff Pollution Prevention and Control Planning." *EPA 1625/R-93/004*, Office of Research and Development, Washington, DC.

Visvanathan, C., Werellagama, D. R. I. B., and Aim, R. B. (1996). "Surface Water Pretreatment Using Floating Media Filter." *J. Environ. Eng.*, 122(1), 25-33.

Wang, G. T., Chen, S., Barber, M. E., and Yonge, D. R. (2004). "Modeling Flow and Pollutant Removal of Wet Detention Pond Treating Stormwater Runoff." *J. Environ. Eng.*, 130(11), 1315-1321.

Waschbusch, R. J., Selbig, W. R., and Bannerman, R. T. (1999). "Sources of Phosphorus in Stormwater and Street Dirt from Two Urban Residential Basins In Madison, Wisconsin, 1994–95." *Water-Resources Investigations Report 99–4021*, U.S. Geological Survey, Middleton, Wisconsin.

Wu, J. S., Holman, R. E., and Dorney, J. R. (1996). "Systematic Evaluation of Pollution Removal by Urban Wet Detention Ponds." *J. Environ. Eng.*, 122(11), 983-988.

Table 1 Freundlich Isotherm Model Constants

Media		Freundlich Model		
Adsorbents	Diameter (mm)	K_F	n	R^2
AOCM _c (clay)	0.85 - 2	3.63	1.54	0.94
AOCM _c (clay)	2 – 4.75	1.05	2.74	0.96
Expanded clay substrate	0.85 - 2	0.018	1.27	0.95
Expanded clay substrate	2 – 4.75	0.0077	1.57	0.98
AOCM _p	2 – 4.75	0.39	3.8	0.96
Pumice substrate	2 – 4.75	0.012	1.2	0.96
AOCM _{pcc}	0.85 - 2	1.32	1.72	0.99
CM _{pcc} , Concrete substrate	0.85 - 2	0.52	1.87	0.96
Bioretention soil media	0.001 - 10	0.18	2.58	0.99
UCF - 1	0.5 – 4.75	0.0027	0.85	0.98
UCF -2	0.85 - 10	0.0009	0.66	0.98
Expanded shale-1	2 - 10	0.06	1.9	0.95
Expanded shale-2	0.45 – 4.5	0.14	1.82	0.98

Table 2 Second Order Potential Driving Kinetic Model Constants

Media		Second Order Potential Driving Kinetic Model		
Media	Diameter (mm)	q_e [mg/g]	K [g/mg-min]	R^2
AOCM _c (clay)	0.85 - 2	0.096	6.09	0.98
AOCM _c (clay)	2 – 4.75	0.093	7.83	0.99
Expanded clay substrate	0.85 - 2	0.013	4.57	0.96
Expanded clay substrate	2 – 4.75	0.03	4.8	0.96
AOCM _p	2 – 4.75	0.11	1.19	0.95
Pumice substrate	2 – 4.75	0.03	0.87	0.97
AOCM _{pcc}	0.85 - 2	0.13	0.51	0.97
CM _{pcc} , Concrete substrate	0.85 - 2	0.13	0.29	0.94
Bioretention soil media	0.001 - 10	0.02	4.67	0.95
UCF - 1	0.5 – 4.75	Not available*		
UCF -2	0.85 - 10	Not available*		
Expanded shale-1	2 - 10	0.03	0.98	0.91
Expanded shale-2	0.45 – 4.5	0.086	0.58	0.95

*The media does not show any adsorption capacity but release certain amount of P.

Table 3 Thomas Model Constants

Media		Thomas Model		
Adsorbents	Diameter (mm)	K_T [L/min-mg]	q_0 [mg/g]	R^2
AOCM _c (clay)	0.85-2	0.0029	1.26	0.94
AOCM _c (clay)	2-4.75	0.0024	0.11	0.85
AOCM _p	2-4.75	0.0014	0.4	0.92
Pumice substrate	2-4.75	5.29	0.00077	0.77
AOCM _{pcc}	0.85-2	0.0021	0.25	0.94
CM _{pcc} , Concrete substrate	0.85-2	0.0022	0.24	0.98
Biofilter Media	0.001 - 10	13.09	0.0024	0.55
UCF -1	0.5 – 4.75	23.62	0.0018	0.48
UCF -2	0.85 - 10	11.23	0.0024	0.81
Shale-1	2 - 10	23.02	0.0021	0.6
Shale-2	0.45 – 4.5	20	0.0018	0.83

Table 4 Breakthrough and Exhaustion Capacity for Phosphorus Adsorption

Adsorbents	Diameter (mm)	X /M _b [mg/g]	X /M _{exh} [mg/g]	V _b [BV]	V _{exh} [BV]
AOCM _c (clay)	0.85-2	0.70	1.36	680	2000
AOCM _p	2-4.75	0.0002	0.25	<1	1600
Pumice Substrate	2-4.75	< 0.0001	0.0046	<1	36
AOCM _{pcc}	0.85 - 2	0.076	0.26	200	955
CM _{pcc}	0.85 - 2	0.056	0.25	120	1075
Bioretention Soil Media	0.001 - 10	< 0.0001	0.012	<1	220
UCF -1	0.5 – 4.75	Phosphorus leaching from media			
UCF -2	0.85 - 10	Phosphorus leaching from media			
Expanded Shale - 1	2 - 10	Phosphorus leaching from media			
Expanded Shale - 2	0.45 – 4.5	< 0.0001	0.0014	<1	12

Note: X / M_b = breakthrough capacity as C / C₀ = 0.1; X / M_{exh} = exhaustion capacity as C / C₀ = 0.9; V_b = number of bed volumes (BV) treated at an effluent breakthrough level of C / C₀ = 0.1; V_{exh} = number of bed volumes (BV) treated at an effluent exhaustion level of C / C₀ = 0.9.

Table 5 Summary of Media Capacity

Media	Adsorption	Kinetics	Breakthrough Capacity	Exhaustion Capacity
AOCM _c (clay) (0.85 - 2 mm)	●	●	●	●
AOCM _c (clay) (2 – 4.75 mm)	●	●	○	◇
Expanded clay substrate (0.85 - 2 mm)	○	○	○	○
Expanded clay substrate (2 – 4.75 mm)	○	○	○	○
AOCM _p	◇	●	○	●
Pumice substrate	○	○	○	○
AOCM _{pcc}	●	●	◇	●
CM _{pcc} , Concrete substrate	●	●	◇	●
Bioretention soil media	○	●	○	○
UCF - 1	○	○	○	○
UCF -2	○	○	○	○
Expanded shale-1	○	○	○	○
Expanded shale-2	○	○	○	○

● High capacity
 ◇ Medium capacity
 ○ Low capacity

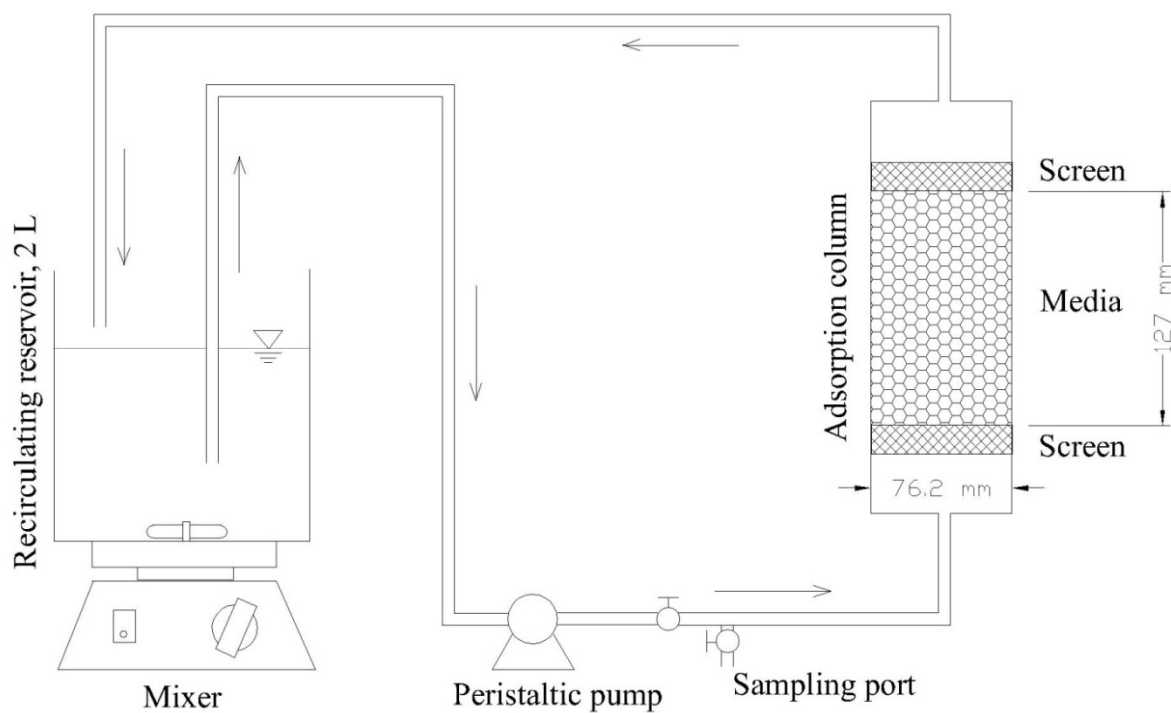


Figure 1 Schematic experimental configuration of TDP adsorption kinetics on adsorbent media

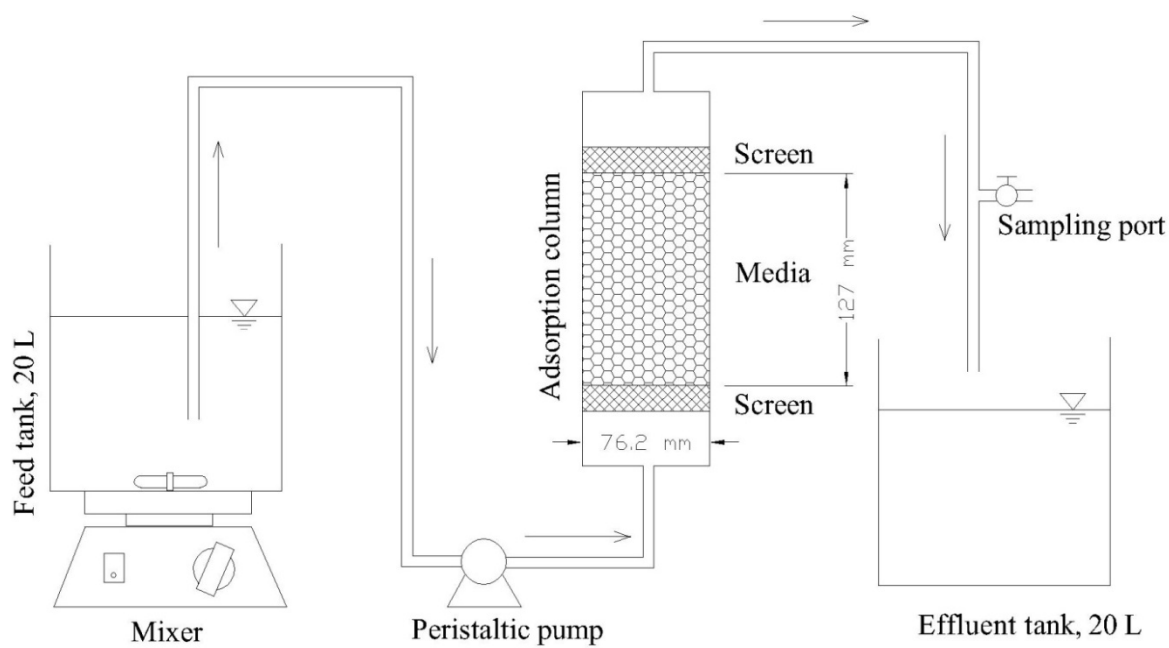


Figure 2 Schematic experimental configuration of TDP adsorption breakthrough on adsorbent media

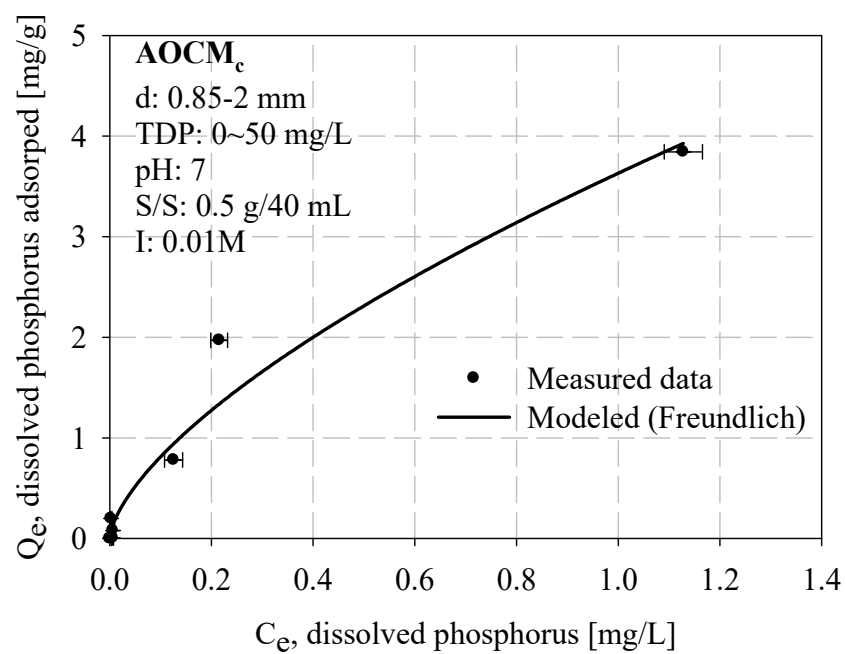


Figure 3 Phosphorus equilibrium isotherm for AOCCMc (0.85 - 2 mm)

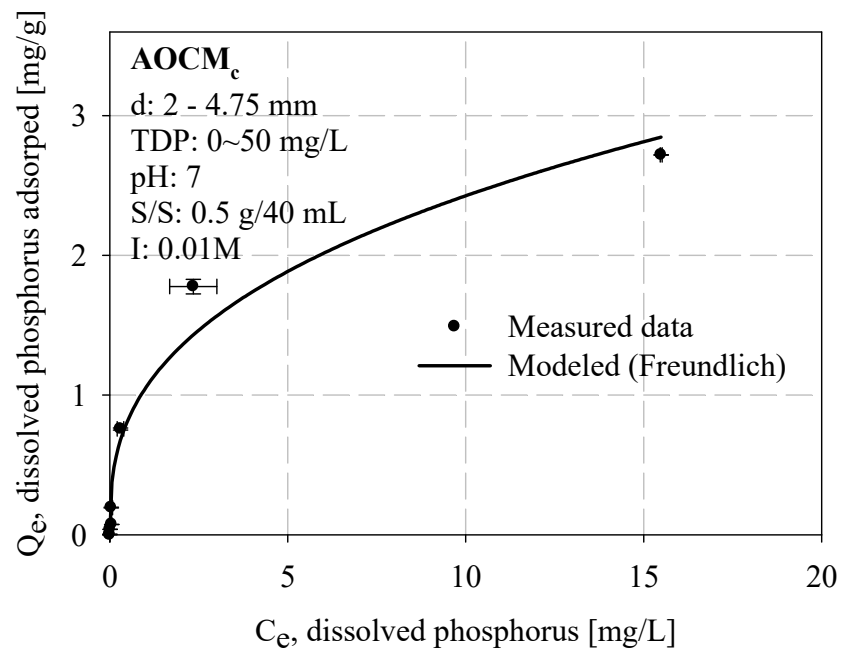


Figure 4 Phosphorus equilibrium isotherm for AOCCMc (2 - 4.75 mm)

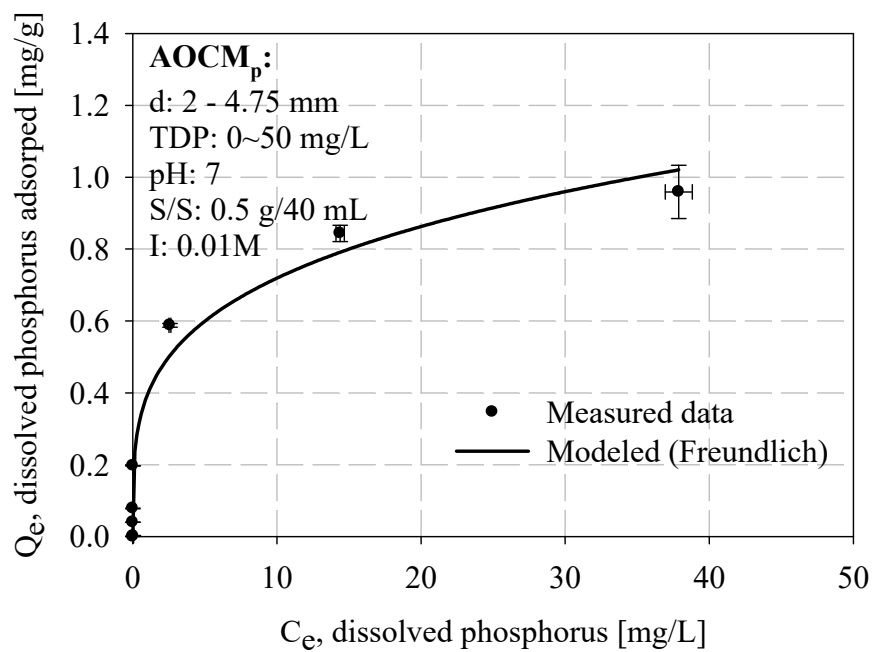


Figure 5 Phosphorus equilibrium isotherm for AOCP_p (2 – 4.75 mm)

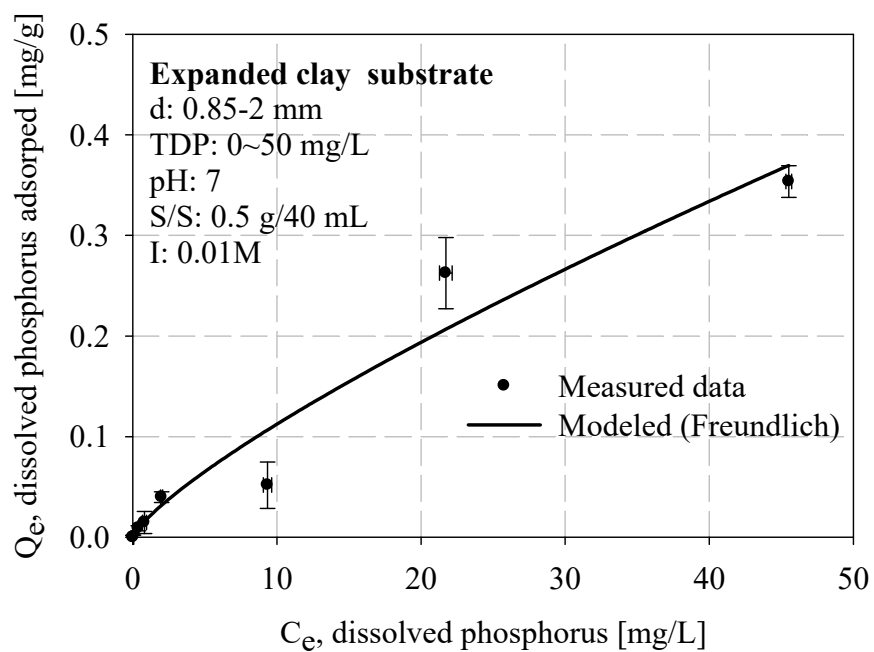


Figure 6 Phosphorus equilibrium isotherm for Expanded clay substrate (0.85 – 2 mm)

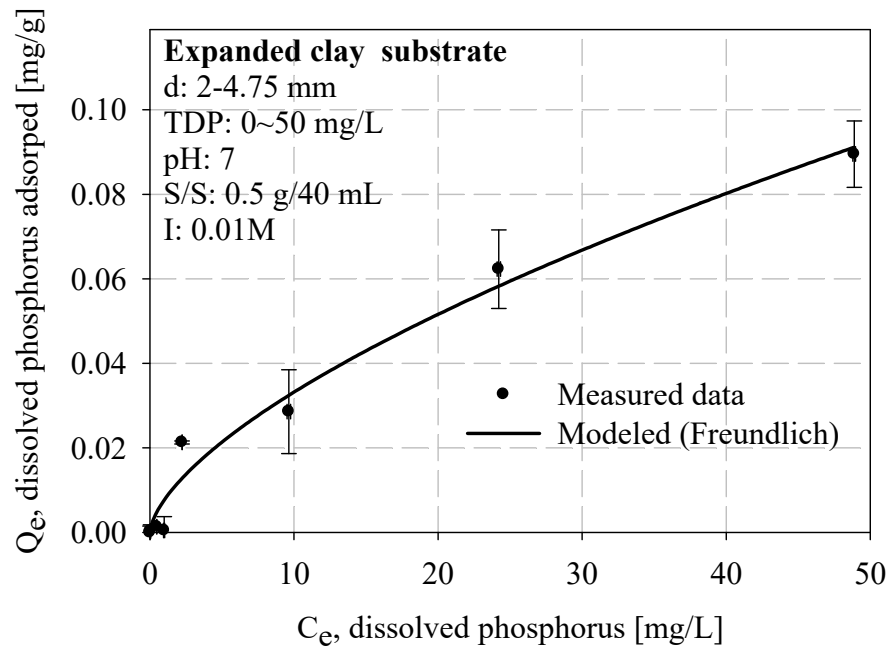


Figure 7 Phosphorus equilibrium isotherm for Expanded clay substrate (2 – 4.75 mm)

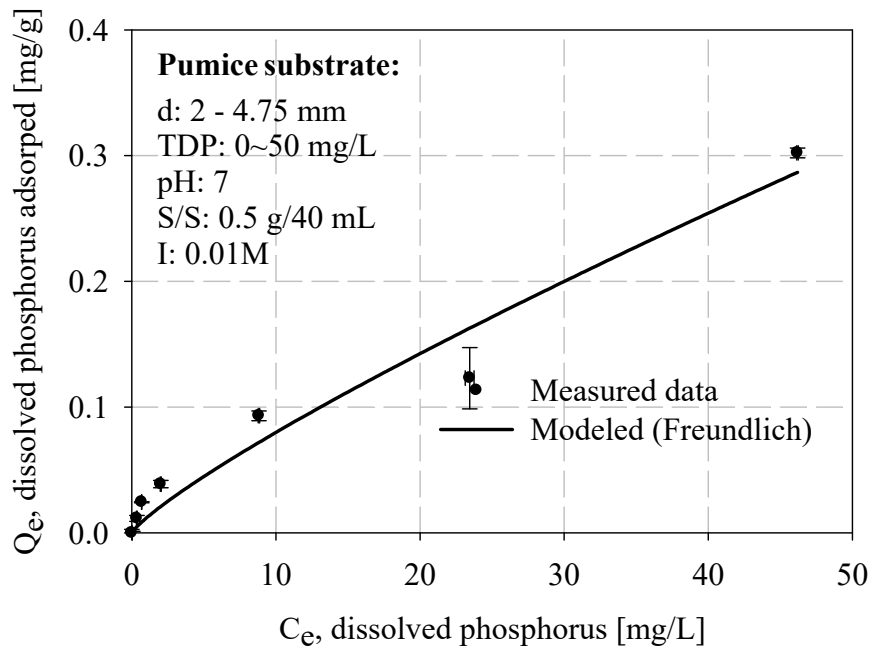


Figure 8 Phosphorus equilibrium isotherm for Pumice substrate (2 – 4.75 mm)

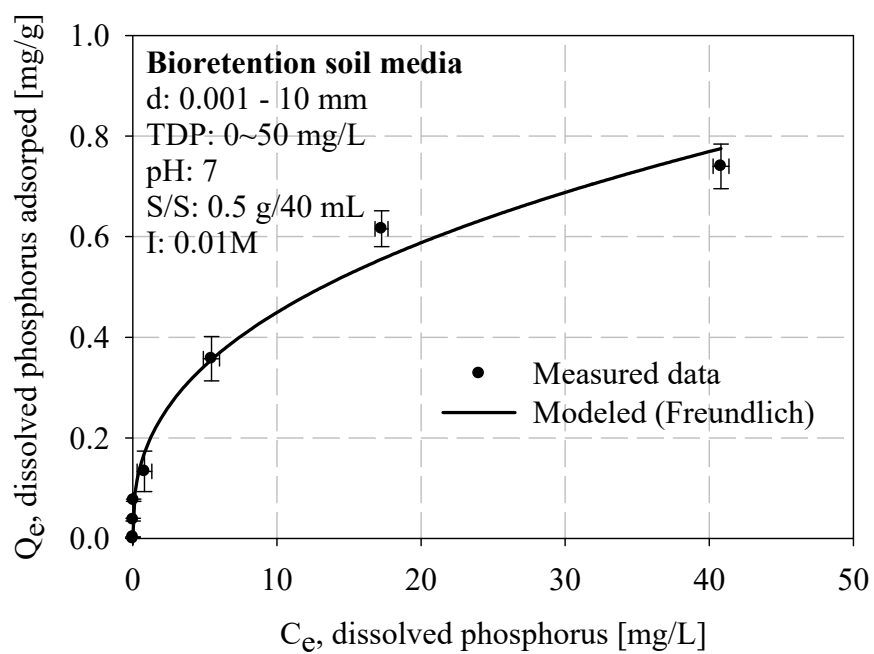


Figure 9 Phosphorus equilibrium isotherm for Bioretention soil media (0.001 – 10 mm)

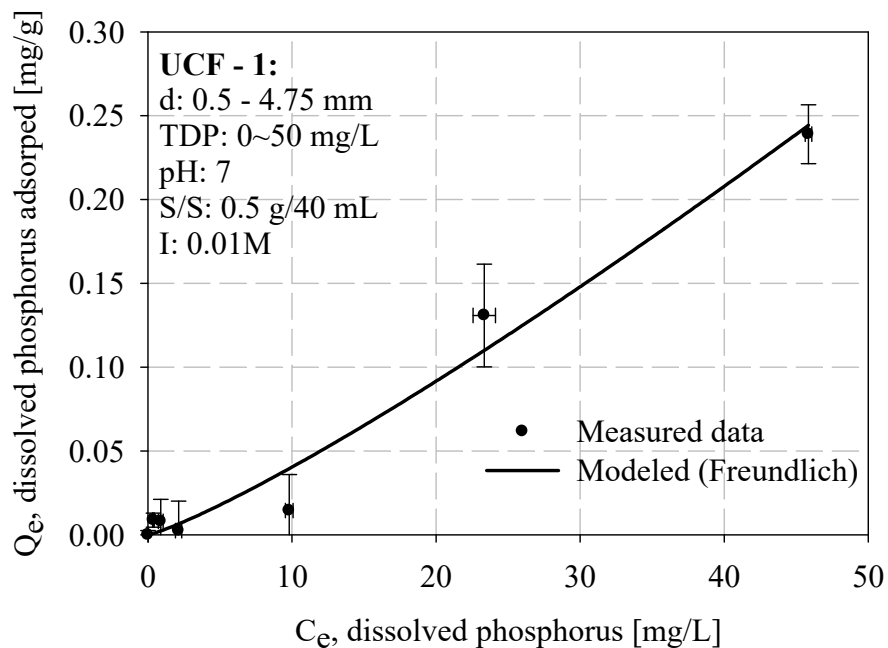


Figure 10 Phosphorus equilibrium isotherm for UCF-1 (0.5 – 4.75 mm)

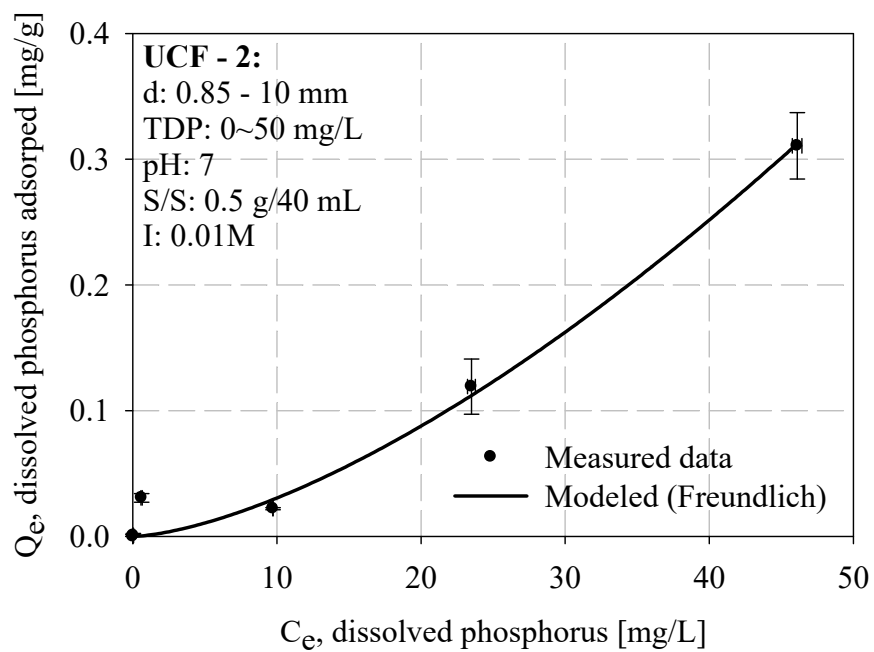


Figure 11 Phosphorus equilibrium isotherm for UCF-2 (0.85 – 10 mm)

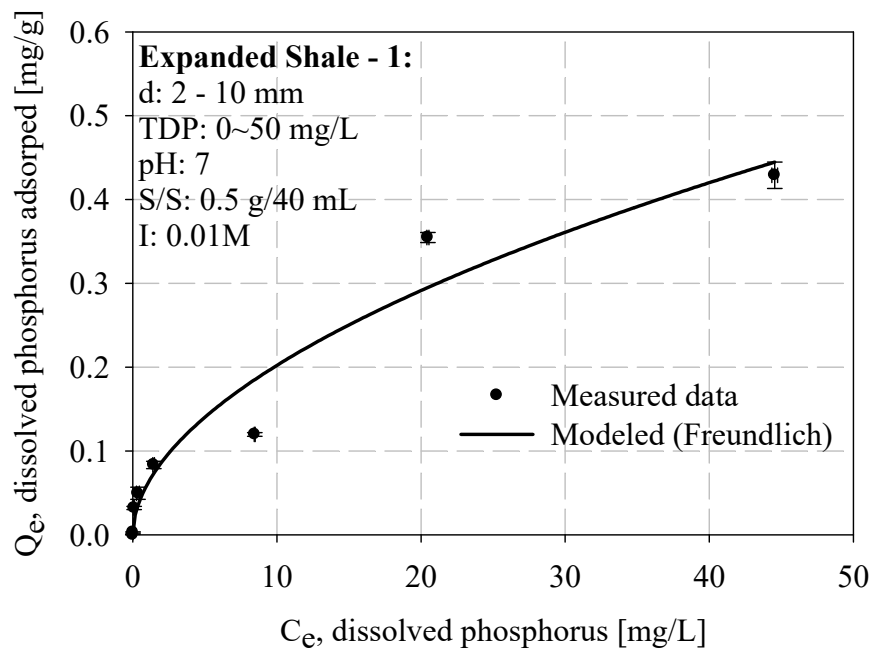


Figure 12 Phosphorus equilibrium isotherm for Expanded Shale-1 (2 – 10 mm)

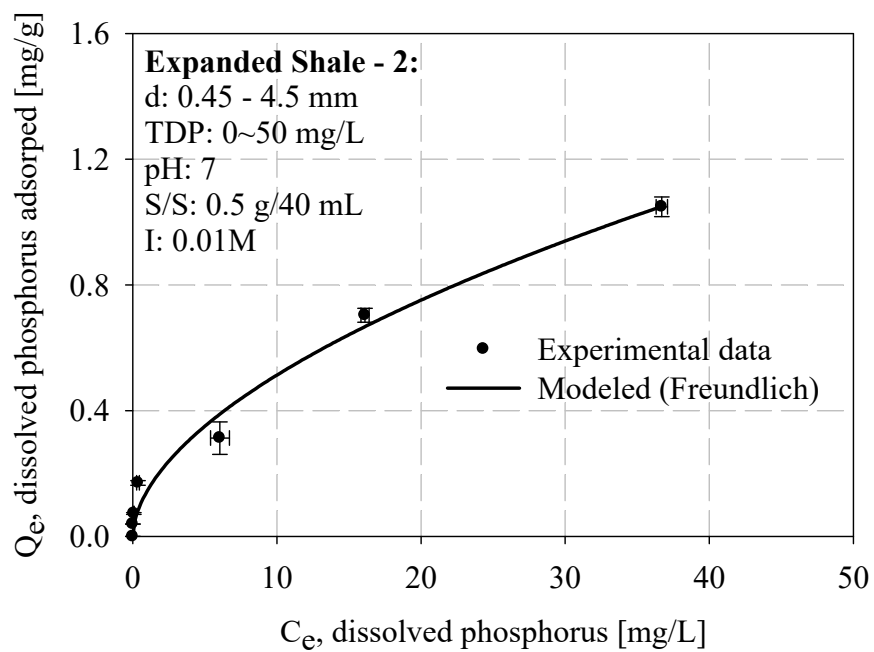


Figure 13 Phosphorus equilibrium isotherm for Expanded Shale-2 (0.45 – 4.5 mm)

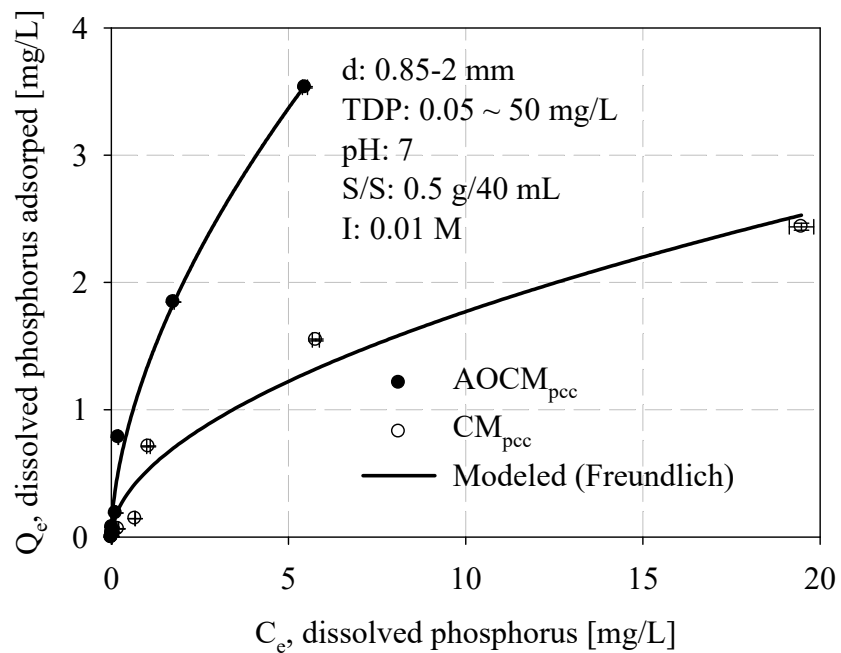


Figure 14 Phosphorus equilibrium isotherm for $AOCP_{pcc}$ and CM_{pcc} (0.85 – 2 mm)

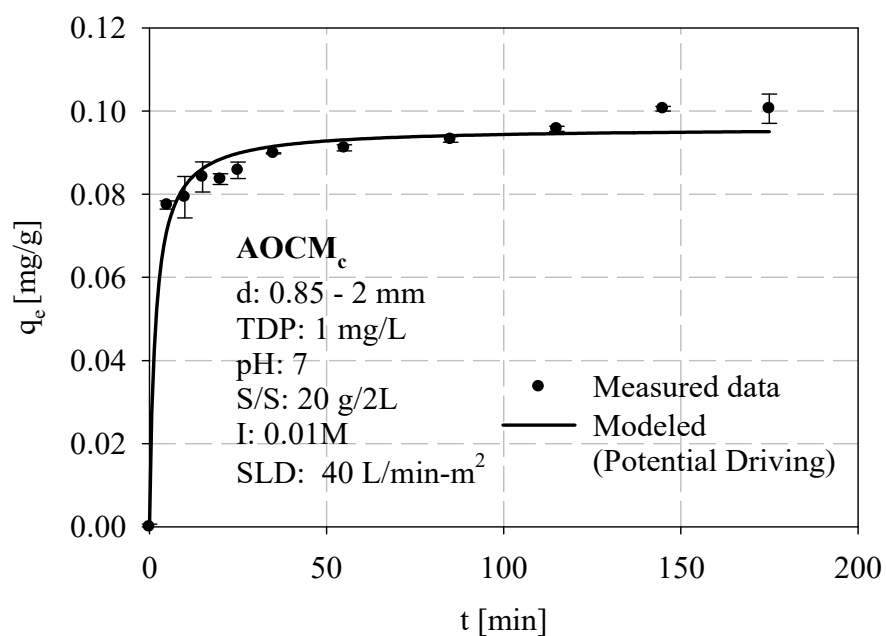


Figure 15 Phosphorus adsorption kinetics for AOCM_c (0.85 - 2 mm)

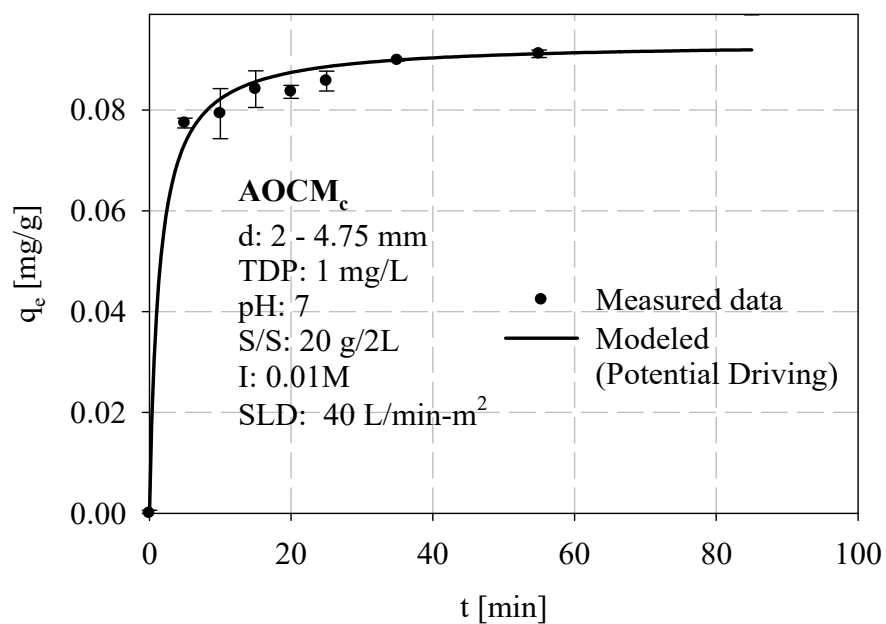


Figure 16 Phosphorus adsorption kinetics for AOCM_c (2 - 4.75 mm)

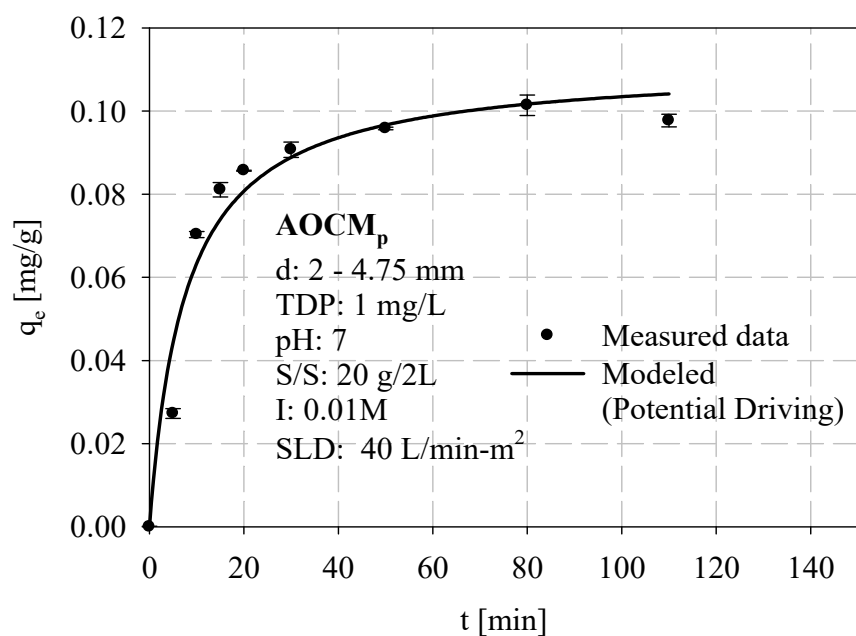


Figure 17 Phosphorus adsorption kinetics for AOCP_m (2 – 4.75 mm)

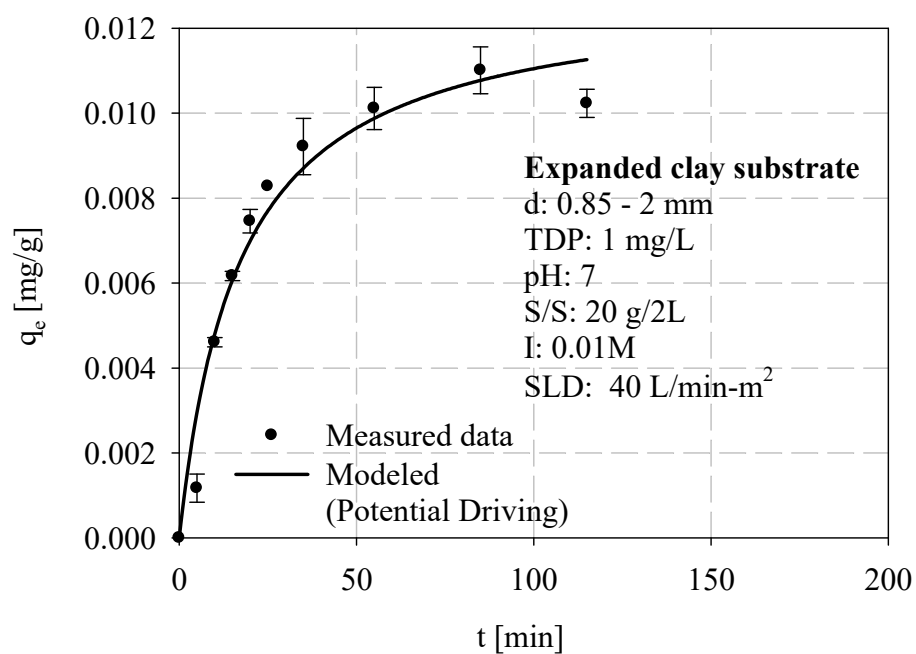


Figure 18 Phosphorus adsorption kinetics for Expanded clay substrate (0.85 – 2 mm)

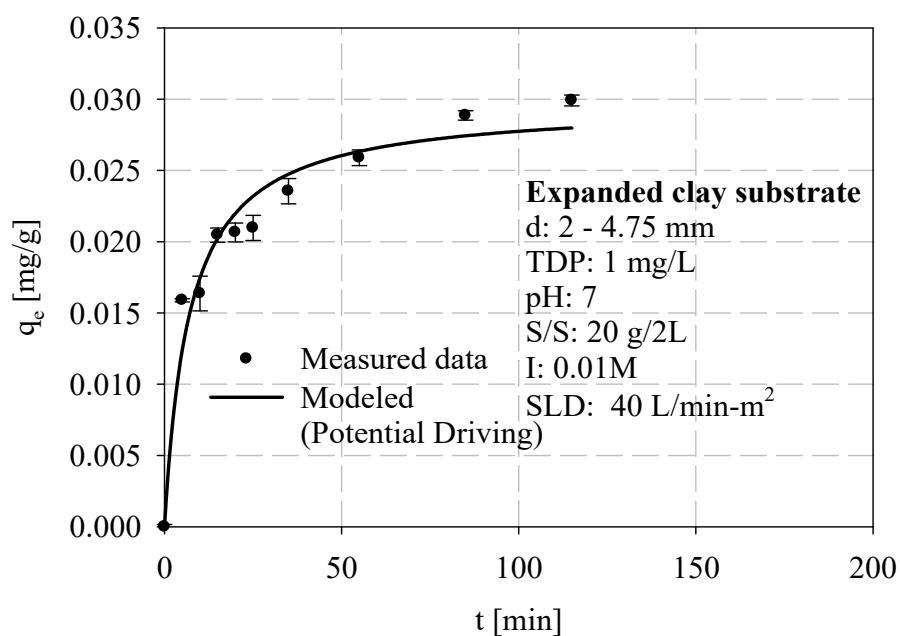


Figure 19 Phosphorus adsorption kinetics for Expanded clay substrate (2 – 4.75 mm)

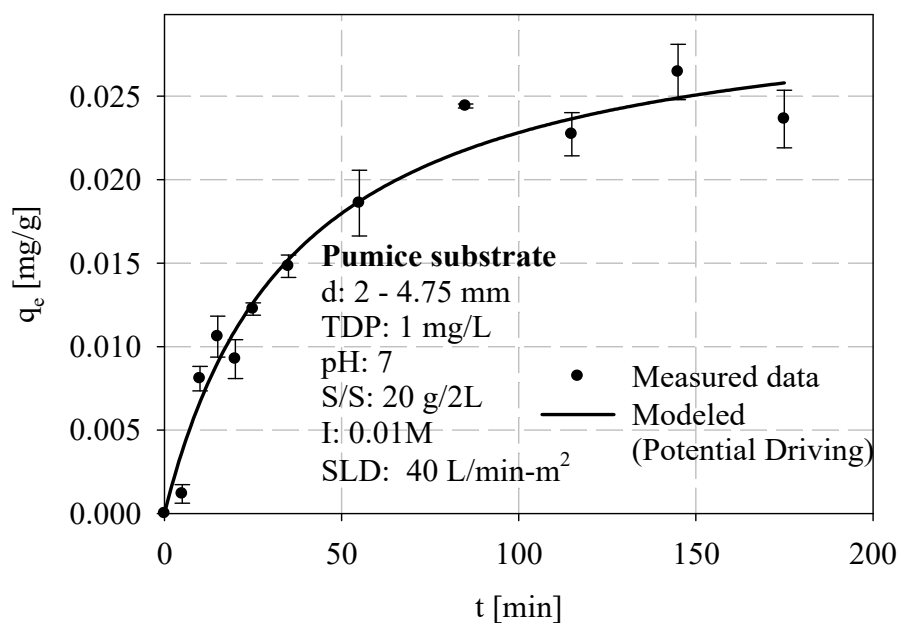


Figure 20 Phosphorus adsorption kinetics for Pumice substrate (2 – 4.75 mm)

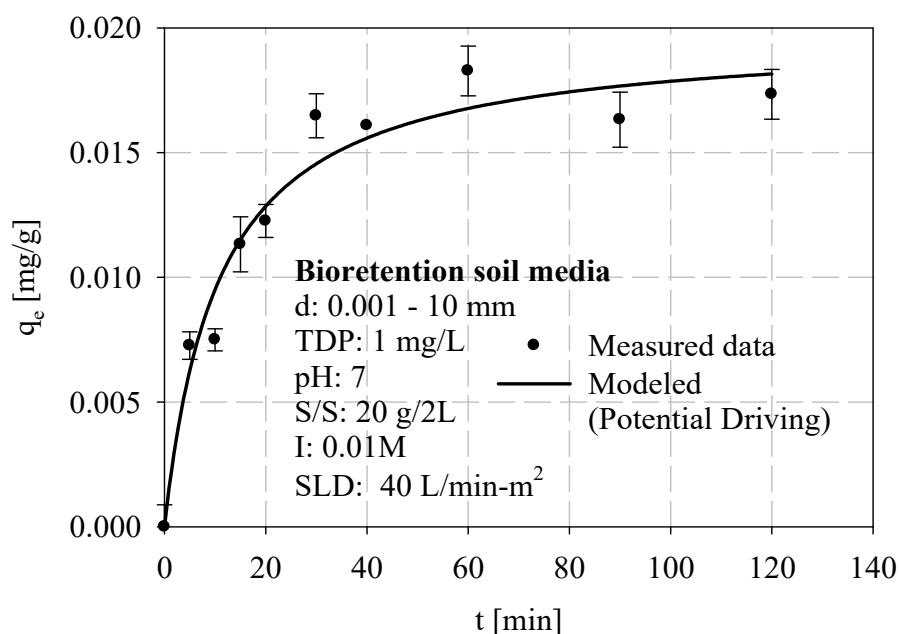


Figure 21 Phosphorus adsorption kinetics for Bioretention soil media (0.001 – 10 mm)

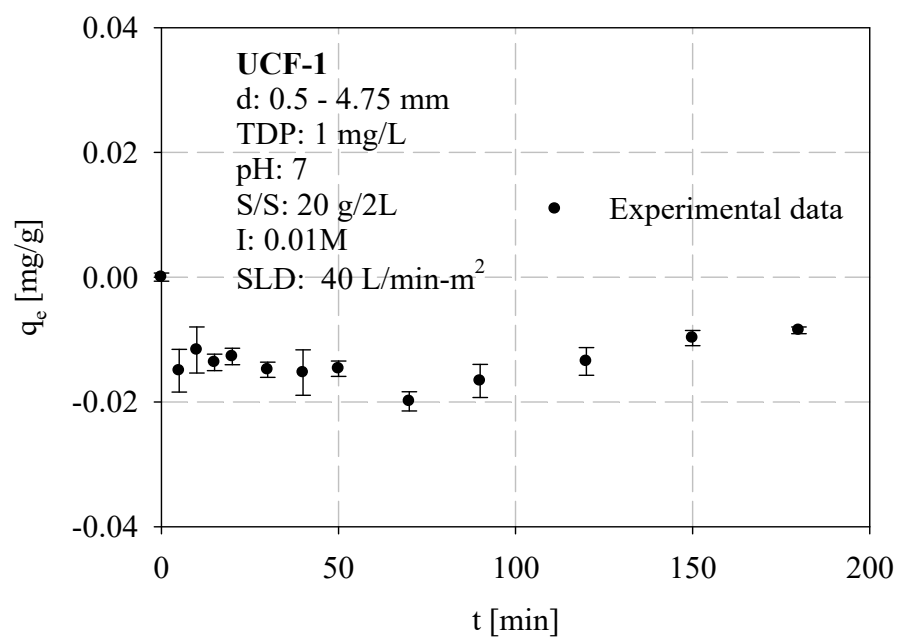


Figure 22 Phosphorus adsorption kinetics for UCF-1 (0.5 – 4.75 mm)
(Experimental data (negative q_e) cannot fit in a pseudo second order model.)

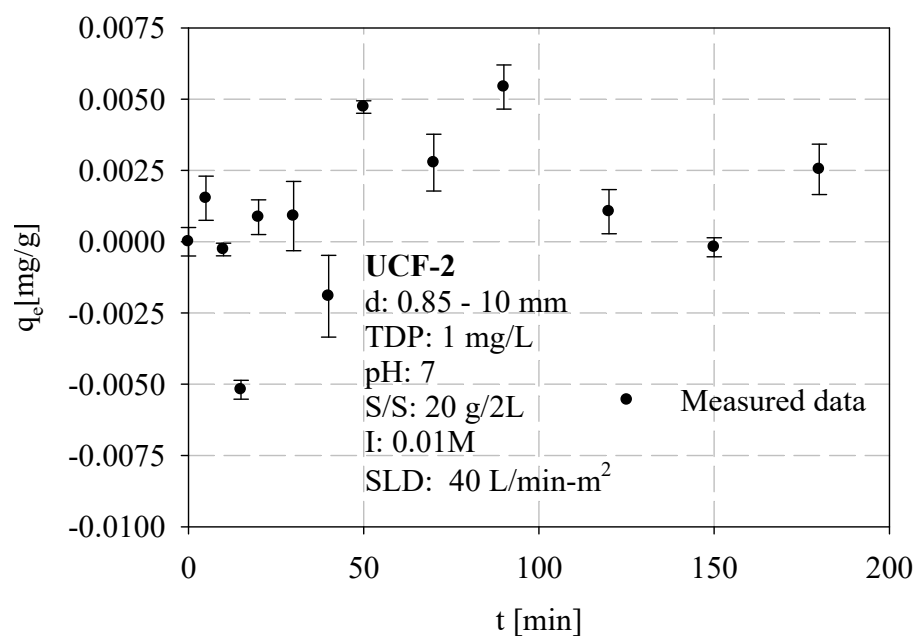


Figure 23 Phosphorus adsorption kinetics for UCF-2 (0.85 – 10 mm)
(Experimental data (negative q_e) cannot fit in a pseudo second order model.)

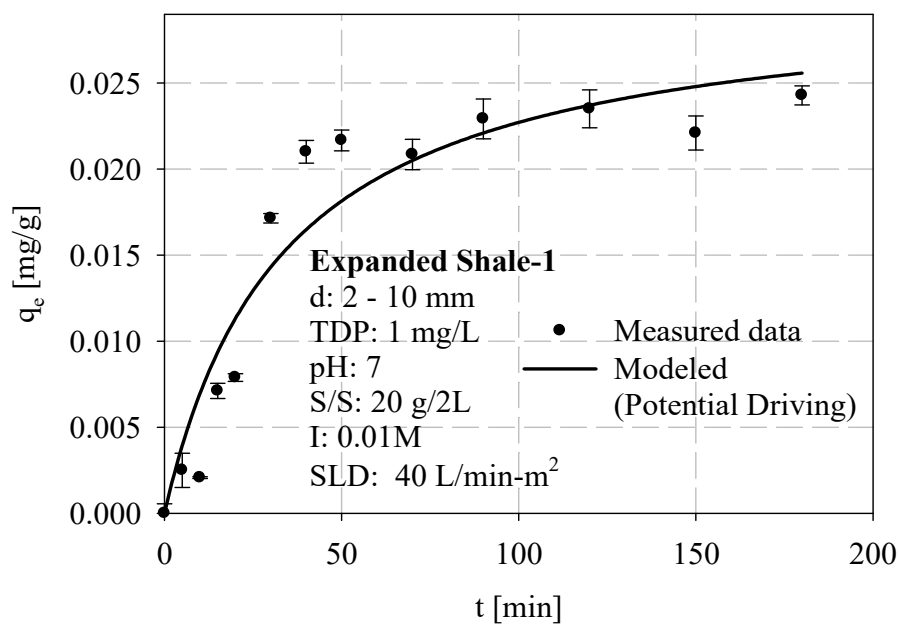


Figure 24 Phosphorus adsorption kinetics for Expanded Shale -1 (2 - 10 mm)

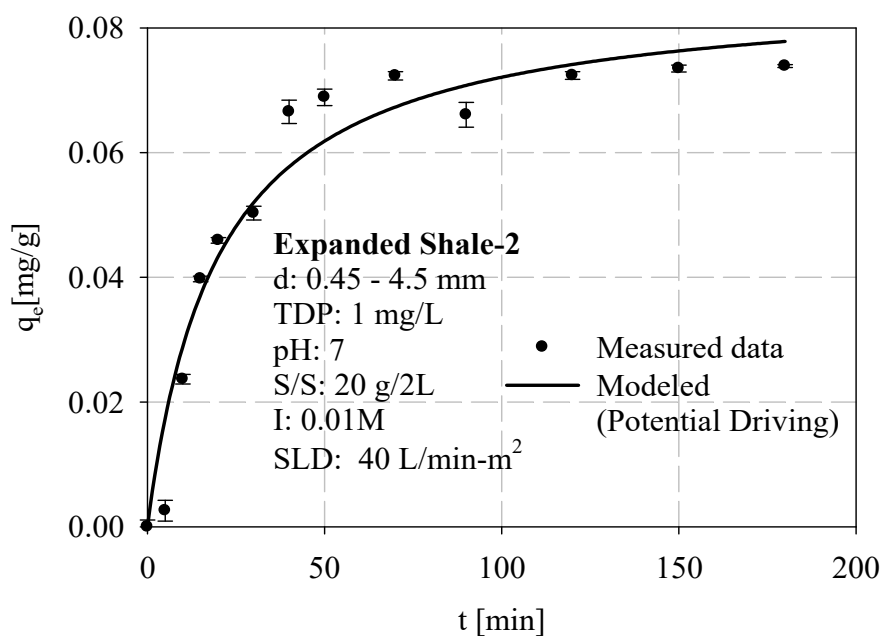


Figure 25 Phosphorus adsorption kinetics for Expanded Shale - 2 (0.45 – 4.5 mm)

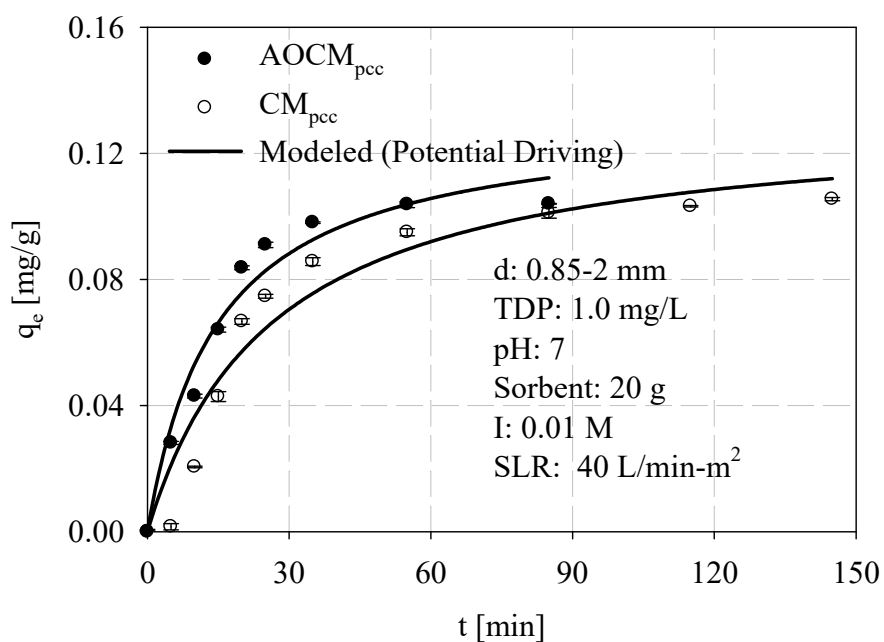


Figure 26 Phosphorus adsorption kinetics for AOCP_{pcc} and CM_{pcc} (0.85 – 2 mm)

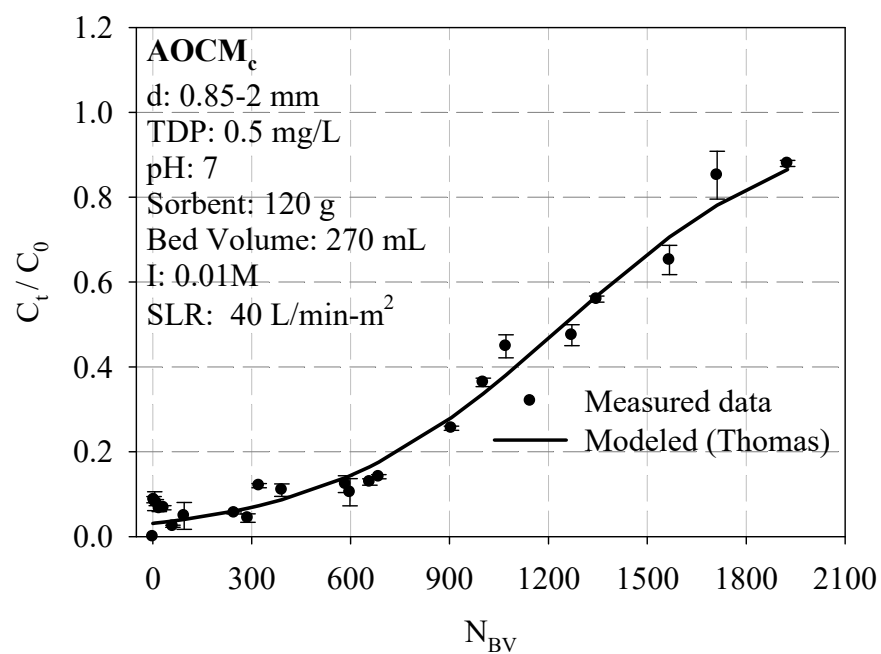


Figure 27 Phosphorus breakthrough test for AOCMc (0.85 – 2 mm)

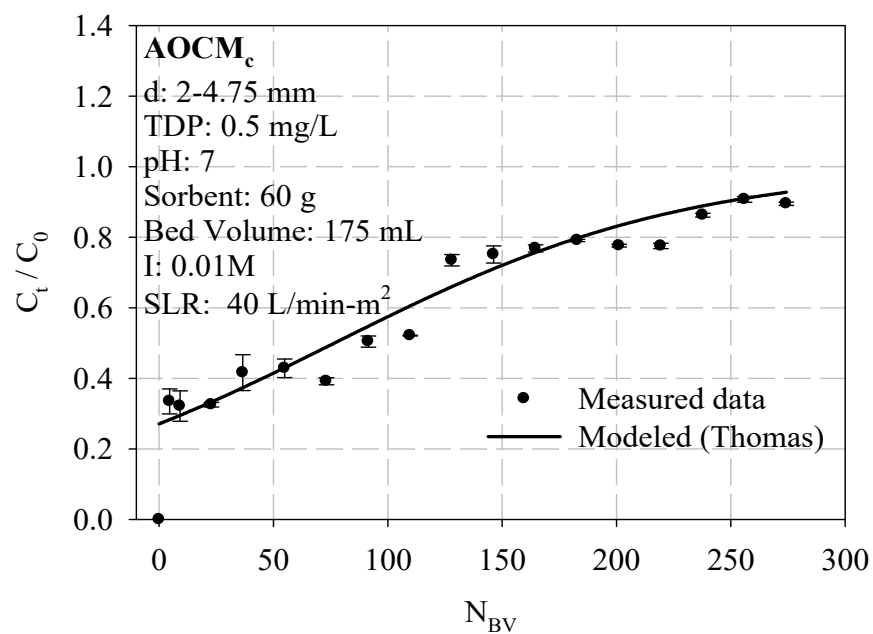


Figure 28 Phosphorus breakthrough test for AOCMc (2 – 4.75 mm)

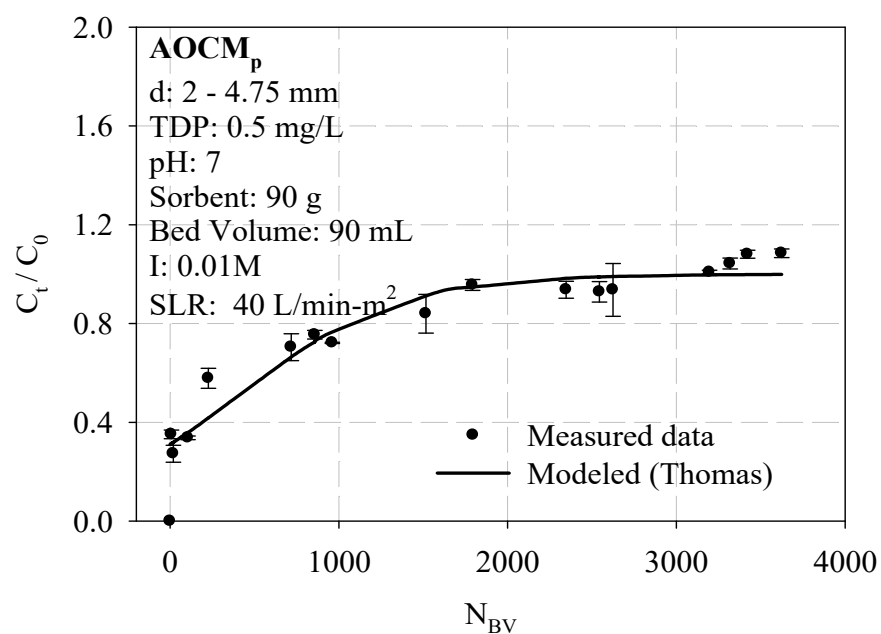


Figure 29 Phosphorus breakthrough test for AOCMP (2 – 4.75 mm)

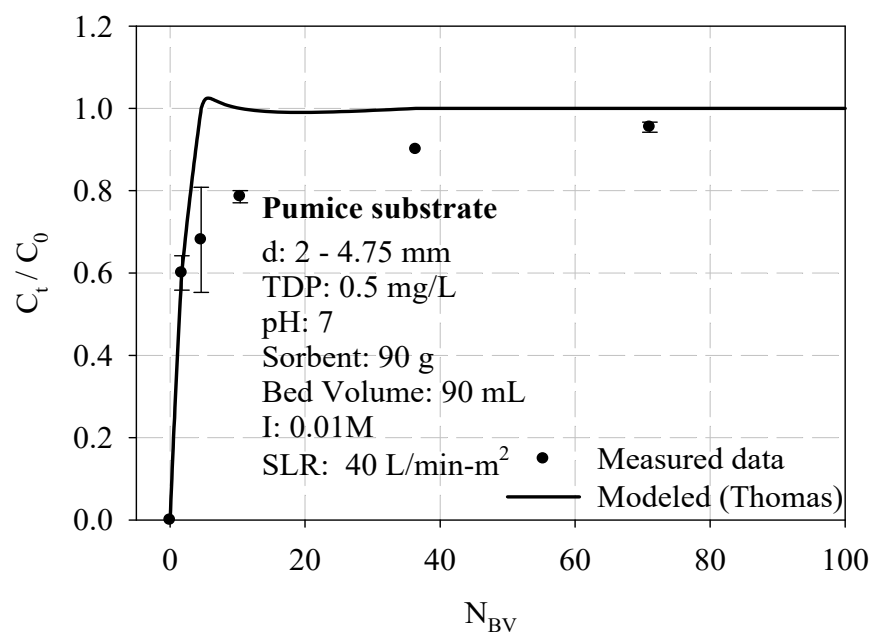


Figure 30 Phosphorus breakthrough test for Pumice substrate (2 – 4.75 mm)

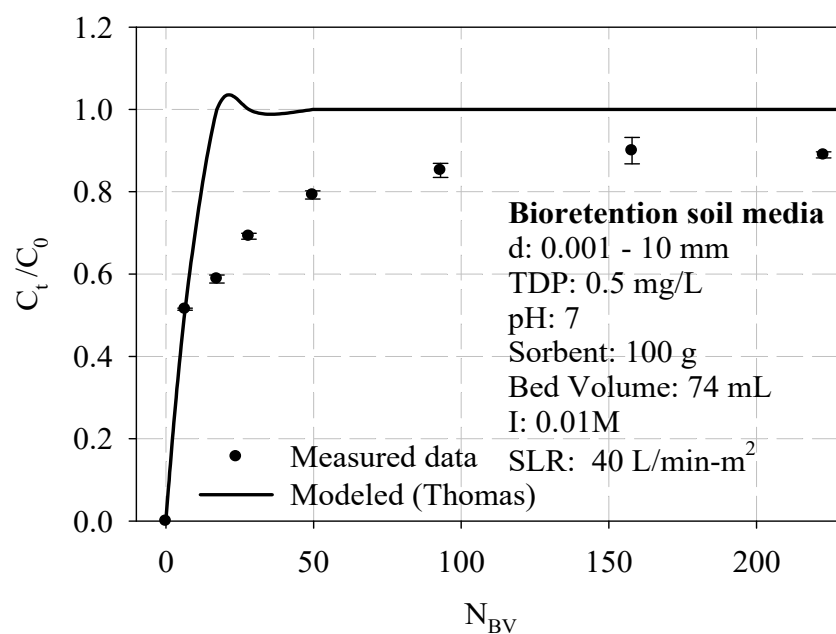


Figure 31 Phosphorus breakthrough test for Bioretention soil media(0.001 – 10 mm)

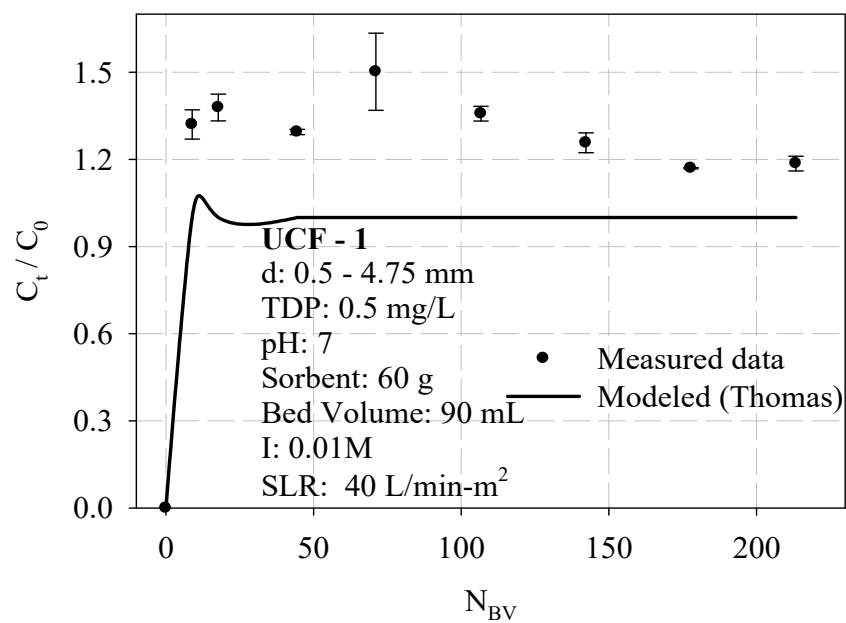


Figure 32 Phosphorus breakthrough test for UCF-1 (0.5 – 4.75 mm)

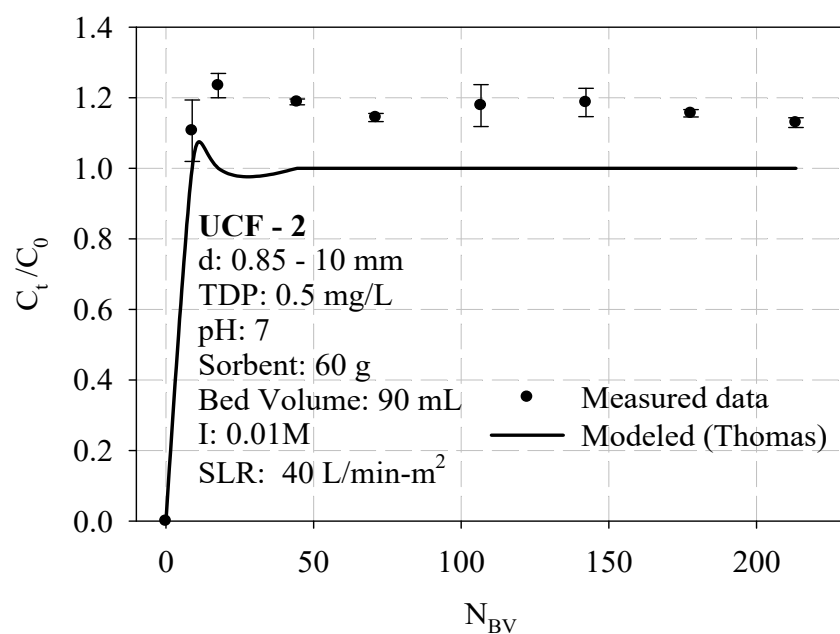


Figure 33 Phosphorus breakthrough test for UCF-2 (0.85 – 10 mm)

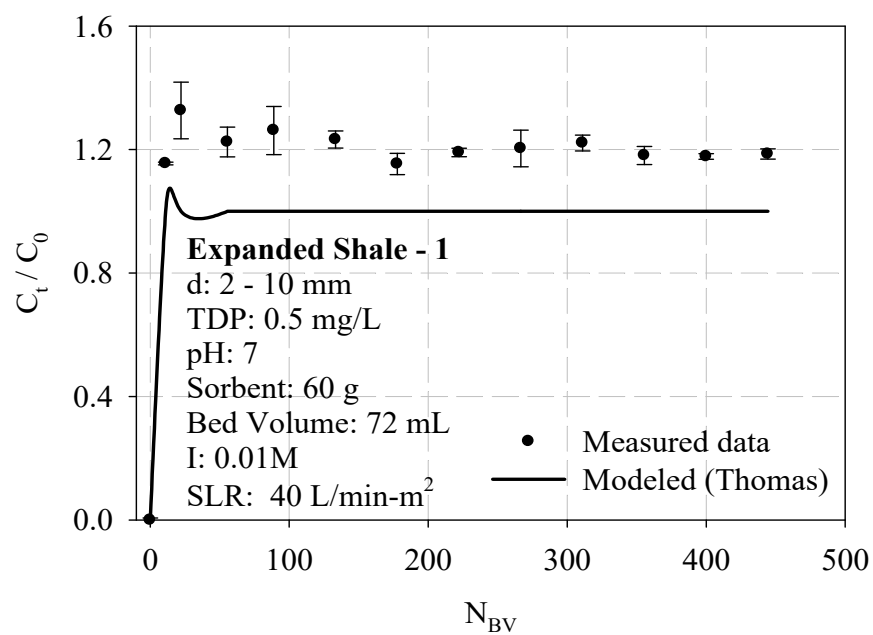


Figure 34 Phosphorus breakthrough test for Expanded Shale-1 (2 – 10 mm)

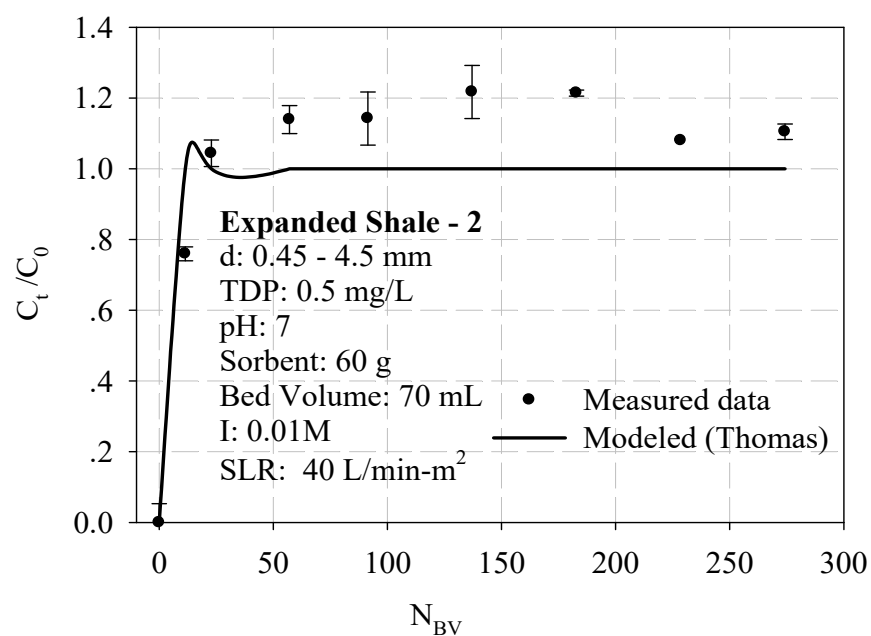


Figure 35 Phosphorus breakthrough test for Expanded Shale - 2 (0.45 – 4.5 mm)

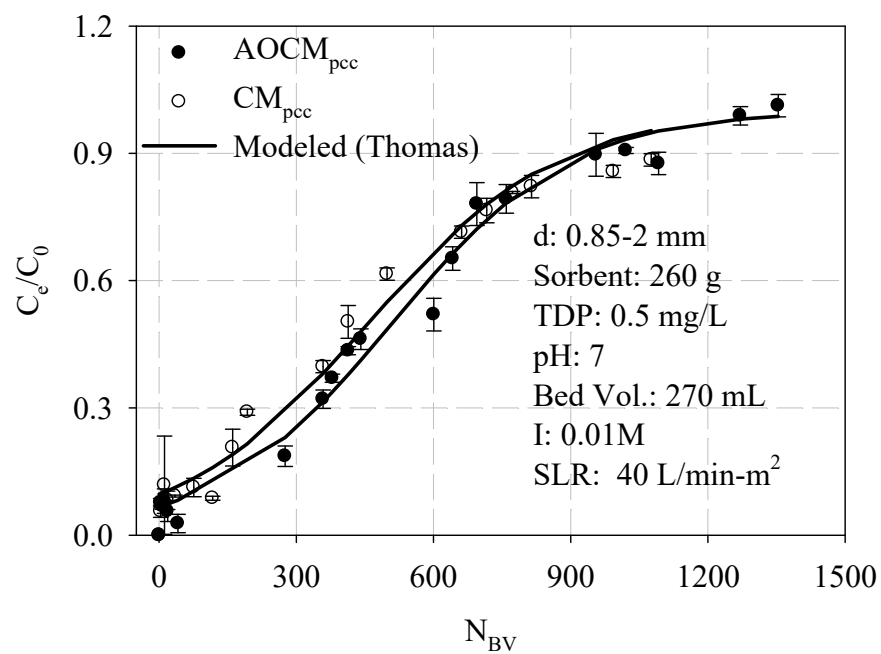


Figure 36 Phosphorus breakthrough test for AOCP_{pcc} and CM_{pcc} (0.85 – 2 mm)

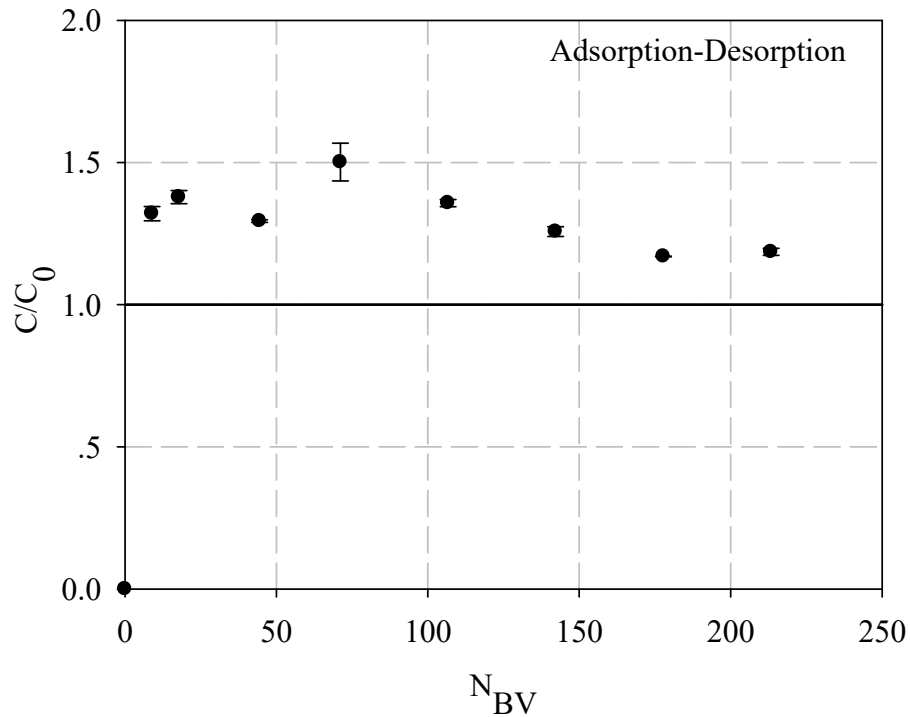


Figure 37 Phosphorus Adsorption-Desorption test for UCF-1 media (0.5 – 4.75 mm). The distance and area between the data and the C/C_0 line = 1.0 represents phosphorus desorption in terms of concentration and mass, respectively.

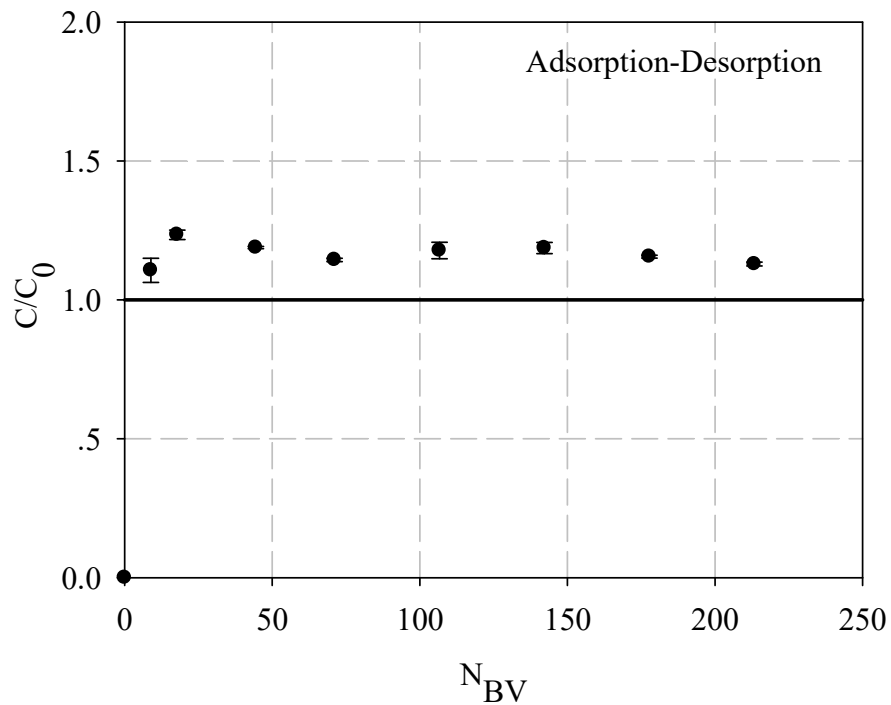


Figure 38 Phosphorus Adsorption-Desorption test for UCF-2 (0.85 – 10 mm). The distance and area between the data and the C/C_0 line = 1.0 represents phosphorus desorption in terms of concentration and mass, respectively.

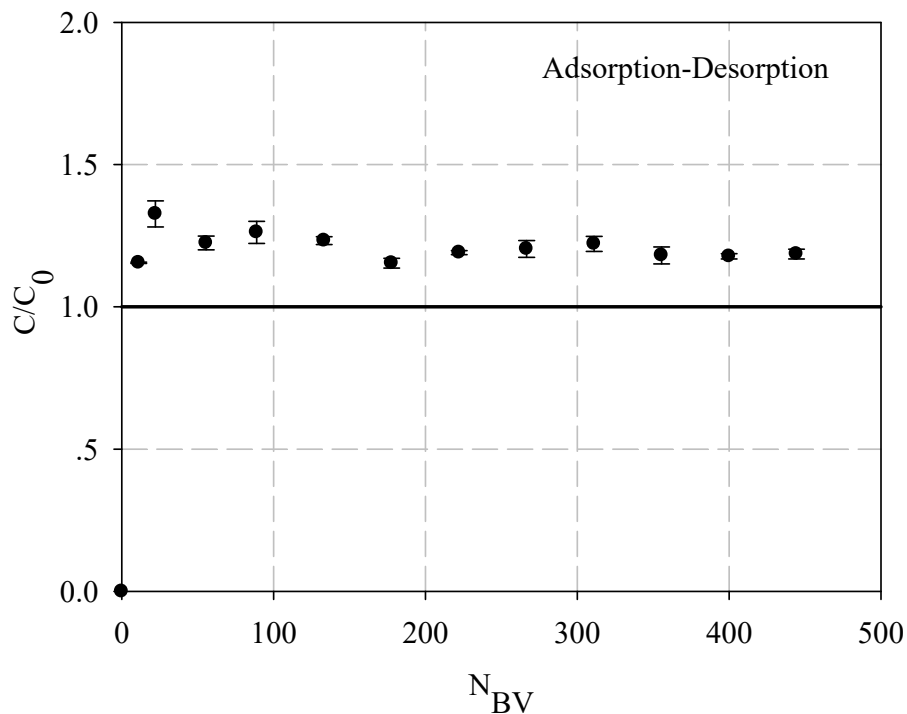


Figure 39 Phosphorus Adsorption-Desorption test for Expanded Shale -1 (2 - 10 mm). The distance and area between the data and the C/C_0 line = 1.0 represents phosphorus desorption in terms of concentration and mass, respectively.

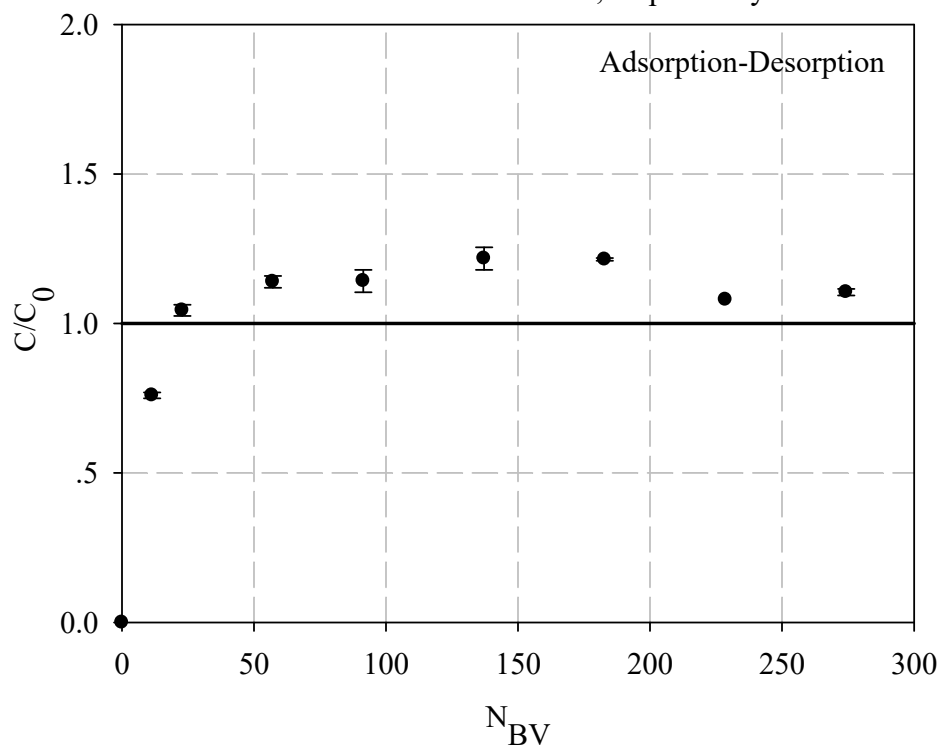


Figure 40 Phosphorus Adsorption-Desorption test for Expanded Shale -2 (0.45 – 4.5 mm). The distance and area between the data and the C/C_0 line = 1.0 represents phosphorus desorption in terms of concentration and mass, respectively.

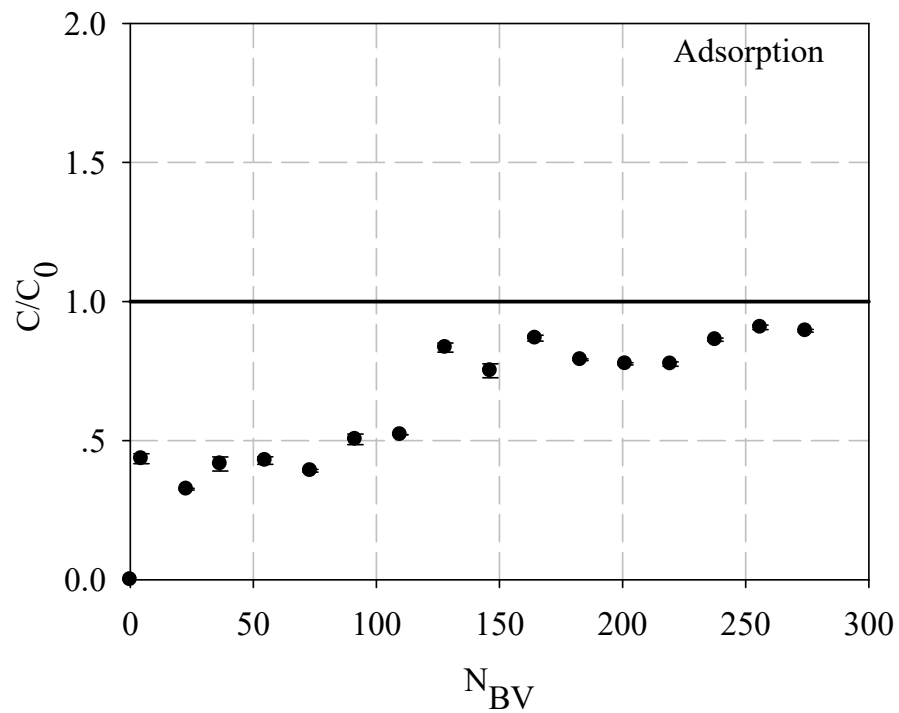


Figure 41 Phosphorus Adsorption test for AOCCM_c (2 – 4.75 mm). This media did not exhibit any desorption and all data are below the C/C_0 line = 1.0; therefore the distance and area between the data and the C/C_0 line = 1.0 represents phosphorus adsorption in terms of concentration and mass, respectively.